

---

Electronic Theses and Dissertations, 2004-2019

---

2016

## Effects of climate change and anthropogenic activities on the Everglades landscape.

Daljit Sandhu  
University of Central Florida, dsandhu@knights.ucf.edu



Part of the [Hydraulic Engineering Commons](#)

Find similar works at: <https://stars.library.ucf.edu/etd>

University of Central Florida Libraries <http://library.ucf.edu>

This Masters Thesis (Open Access) is brought to you for free and open access by STARS. It has been accepted for inclusion in Electronic Theses and Dissertations, 2004-2019 by an authorized administrator of STARS. For more information, please contact [STARS@ucf.edu](mailto:STARS@ucf.edu).

---

### STARS Citation

Sandhu, Daljit, "Effects of climate change and anthropogenic activities on the Everglades landscape." (2016). *Electronic Theses and Dissertations, 2004-2019*. 5337.  
<https://stars.library.ucf.edu/etd/5337>

**EFFECTS OF CLIMATE CHANGE  
AND ANTHROPOGENIC ACTIVITIES  
ON THE EVERGLADES LANDSCAPE**

by

DALJIT SANDHU  
B.S. University of Central Florida, 2014

A thesis submitted in partial fulfillment of the requirements  
for the degree of Master of Science  
in the Department of Civil, Environmental, and Construction Engineering  
in the College of Engineering and Computer Science  
at the University of Central Florida  
Orlando, Florida

Fall Term  
2016

Major Professor: Arvind Singh

© 2016 Daljit Sandhu

## ABSTRACT

The Everglades has been experiencing major changes, both climatic and anthropogenic, such that the landscape is experiencing additional stresses and forcings leading it away from its natural equilibrium. The land within and surrounding the Everglades has undergone severe modifications that may have detrimental effects on wildlife and natural features, such as rivers and landscape connectivity. Here in this study, the main focus is on understanding and quantifying hydrologic and geomorphic signatures of climatic and anthropogenic changes on the Everglades landscape. For this, in particular, available data on natural hydrological processes was used, such as rainfall, groundwater elevation, streamflow as well as surface elevations and satellite images for three different regions. These regions are categorized as forested, urban (nearby Everglades regions) and transition (in between forested and urban regions). The results show distinct differences in the statistics of observed hydrologic variables for the three different regions. For example, the probability distribution functions (PDFs) of groundwater elevation for the case of urban region show a shift in mean as well as lower asymmetry as compared to forested regions. In addition, a significant difference in the slopes between smaller and larger scales of the power spectral densities (PSDs) is observed when transitioning from forested to urban. For the case of the streamflow PDFs and PSDs, the opposite trends are observed. Basin properties extracted from digital elevation models (DEMs) of the Everglades reveal that drainage densities increase when moving from the urban to the forested sub-regions, highlighting the topographic and land use/land cover changes that the Everglades has been subjected to in recent years. Finally, computing the interarrival times of extreme (>95th percentile) events that suggest power-law behavior, the changes in power-law exponents of the hydrologic processes further

highlights how these processes differ spatially and how the landscape has to respond to these changes. Quantifying these observed changes will help develop a better understanding of the Everglades and other wetlands ecosystems for management to future changes and restoration.

## **ACKNOWLEDGMENTS**

I would like to take this opportunity to thank all the people who have helped me complete my graduate studies. I could not have done this without the support of all these people. I would also like to extend my thanks to my adviser, Dr. Arvind Singh, for presenting me this unique opportunity to take on this research study, and for allowing me to be a part of the Center for Hydroscience Analysis, Modeling and Predictive Simulations (CHAMPS) Lab. I want to thank Drs. Dingbao Wang and Stephen Medeiros for serving on my committee, for helping me in my research, and for teaching me a lot throughout the past few years. I definitely gained a lot of understanding in both my undergraduate and graduate programs. I am also grateful to all the other professors I have taken in the past that helped contribute to my understanding of civil engineering.

In addition, I would like to thank all members, past and present, of the CHAMPS Lab for being supportive and positive. I am grateful to have served as an officer for the International Association for Hydro-Environment Engineering and Research (IAHR). Through this experience, I have participated in seminars and led some workshops related to engineering. Also, I have been able to attend a conference to present my research. I feel that this experience truly helped me grow better as an individual and professionally as well.

Lastly, I could not have done any of this without the support of my family. They have helped me every step of the way and always provided me with encouragement. I will always be eternally grateful for their unconditional support.

## TABLE OF CONTENTS

LIST OF FIGURES .....	viii
LIST OF TABLES .....	xii
CHAPTER 1: INTRODUCTION .....	1
1.1 Study Area .....	3
CHAPTER 2: LITERATURE REVIEW .....	6
2.1 Sediment Transport and Nutrient Concentration Observations .....	7
2.2 Effects of Sea Level Rise and Nitrogen Loading on Coastal Wetlands .....	8
2.3 Vegetation Characteristics .....	9
2.4 Landscape Feedbacks and Connectivity .....	11
2.5 Quantifying Groundwater Variations .....	13
2.6 Streamflow Alterations .....	14
CHAPTER 3: METHODOLOGY .....	16
CHAPTER 4: RESULTS AND DISCUSSION.....	21
4.1 Variability as a Function of Scale.....	34
4.2 Mean, Variance, and Asymmetry as a Function of Scale .....	43
4.3 Interarrival Time .....	49
4.4 Effect of changing hydrology on river networks .....	53
CHAPTER 5: CONCLUSION .....	58

LIST OF REFERENCES ..... 61



## LIST OF FIGURES

- Figure 1 – Locations of the different USGS stations used in this study along with their notations. From the figure, squares represent stations in the forested area. X's denote stations in the transition area, and triangles denote stations in the urban area. The sample locations depicted as light blue stars denote where the Everglades experienced minor geomorphic changes over time. .... 5
- Figure 2 – Stream network in south Florida. Also, three sample watersheds for the urban, transition, and forested sub-regions are mapped out. .... 20
- Figure 3 – Sample local geomorphology of the Everglades for two different locations (shown in right and left panels) and two different instant of times corresponding to years 1994-5 (top panels) and year 2014 (bottom panels). Examples of changes in local geomorphology are highlighted in yellow. For example, in (a) addition of minor streams or water bodies and changes in channel geometry can be seen. In (b) over time, at the highlighted locations, minor streams and other features no longer exist. These images correspond to points A and B, indicated in Figure 1. .... 23
- Figure 4 – Sample time series plots for daily (a) rainfall,  $R(t)$ , (b) groundwater elevation,  $G(t)$ , and (c) streamflow,  $Q(t)$ .  $R(t)$ ,  $G(t)$ , and  $Q(t)$  correspond to stations U4 (red), U5 (yellow), and U5 (green) from Figure 1a respectively. Note that all the time series are shown for similar time periods for visual comparison, however, longer time series exist and were analyzed for  $G(t)$  and  $Q(t)$ . cms in part (c) represents cubic meter per second. .... 26

Figure 5 – Randomly selected locations where groundwater elevation (left column) and streamflow (right column) experience changes in mean and variance in their time series, highlighting effects of climate change. All these gauges are located in the forested sub-region..... 27

Figure 6 – Probability density functions (PDFs) for rainfall (a), groundwater elevation (b), and streamflow (c). U, T, and F denote urban, transition, and forested sub-regions, respectively. For streamflow, the PDFs are normalized using  $(Q-Q_{\min})/(Q_{\max}-Q_{\min})$ , since streamflow is a function of basin size..... 28

Figure 7 – PDF increments for rainfall (a), groundwater elevation (b), and streamflow (c). Note the asymmetry in the groundwater elevation and streamflow plots. Rainfall PDFs show symmetric behavior. Also note that these PDFs were computed at a scale of 1 day. The insets show the ensemble averages of the increment PDFs for each sub-region. The x-axes represent standardized increments computed using  $(x-\mu)/\sigma$ . ..... 31

Figure 8 – Quantile-Quantile (QQ) plots of each sub-region paired to another sub-region. In each case, the QQ plots form a straight line, indicating that the sample data collected were drawn from the same distributions..... 32

Figure 9 – PDF increments for rainfall (top), groundwater elevation (center), and streamflow (bottom) with a scale equal to 365 days. The insets show the ensemble average of the PDF increments for each sub-region. Like Figure 7, the increments for streamflow are standardized. Notice how these PDFs are more symmetric compared to Figure 7. ... 33

Figure 10 – Average power spectral densities plotted with its error (shown as  $\pm 1$  standard deviation) for rainfall. The top, center, and bottom plots represent the urban, transition, and forested sub-regions, respectively..... 36

Figure 11 – Average power spectral densities plotted with its error (shown as  $\pm 1$  standard deviation) for groundwater elevation. The top, center, and bottom plots represent the urban, transition, and forested sub-regions, respectively..... 40

Figure 12 – Average power spectral densities plotted with its error (shown as  $\pm 1$  standard deviation) for streamflow. The top, center, and bottom plots represent the urban, transition, and forested sub-regions, respectively..... 41

Figure 13 – Superimposed power spectral density plots as is (top row), and shifted by several decades (bottom row). Notice the scaling nature of the plots changes as one moves from urban to forested and vice-versa. .... 42

Figure 14 – Average absolute mean across several scales for rainfall (top), groundwater elevation (center), and streamflow (bottom). .... 46

Figure 15 – Average variance across several scales for rainfall (top), groundwater elevation (center), and streamflow (bottom). .... 47

Figure 16 – Average asymmetry (third moment) index across several scales for rainfall (top), groundwater elevation (center), and streamflow (bottom). The insets show the normalized versions of the periodicities that appear in the original plots for groundwater and streamflow..... 48

Figure 17 – Five (left column) and ninety-five (right column) percentile PDFs for a) rainfall, b) groundwater elevation, and c) streamflow with power law fits for each area. .... 51

Figure 18 – Slope PDFs of the sample watersheds for each corresponding area. These particular basins are shown in Figure 2..... 57

## LIST OF TABLES

Table 1 – Gauges and their properties used in this study. ....	19
Table 2 – Power-law exponents of the interarrival PDFs listed from Figure 17. ....	52
Table 3 – Averaged basin and stream order characteristics for each sub region. ....	56

## CHAPTER 1: INTRODUCTION

The Everglades has been experiencing drastic changes over the past few decades due to both natural and anthropogenic changes that have altered the landscape's stability and heterogeneity as well as habitat diversity (Larsen et al., 2009; Noe et al., 2009, Larsen et al., 2011). These changes are observed, for e.g., in sediment and nutrient dynamics, changing patterns of ridges, sloughs and tree islands, nitrogen loading and vegetation characteristics. Understanding and quantifying different features and characteristics of the Everglades landscape under change can help us emphasize the importance of maintaining its ecosystem in equilibrium as well as predicting its response to future climate change and human intervention.

It has been argued that the natural landscapes are constantly adjusting to their surroundings, i.e., landscapes are reorganizing themselves so that a natural balance is achieved and maintained at all times (Carpenter and Brock, 2006; Erwin, 2009; Nourani et al., 2015; Singh et al., 2015; Abed-Elmdoust et al., 2016). These adjustments occur more often when landscapes are easily prone to instability. While these changes can occur naturally, in some instances, human activity can be an external force or driver that causes instability and propagates a landscape transition (Scheffer et al., 2001). For example, from a historical standpoint, freshwater from Lake Okeechobee flowed south to the Everglades and as freshwater entered the wetlands ecosystems, it counteracted any increase in salinity in the coastal regions (Chambers et al., 2015). Today, canals and dams redirect the flow of water, adversely affecting the landscape. Another example of a large ecosystem transition is climate change (Carpenter and Brock, 2006).

Several studies have focused on investigating the changes in the dynamics of physical features and processes of the Everglades system. For example, Larsen et al. (2011) suggested

that change in the sediment dynamics impacts topography, ecosystems, and restoration efforts. Noe et al. (2011) argued that the dominant pattern of alternating peat-based ridges and sloughs present in the pre-drainage Everglades is altered by recent human activities and current hydrologic conditions in Everglades are not conducive to maintaining this ridge-slough pattern (see also Davis et al., 1994, Sklar et al., 2002; Ogden, 2005). More recently, Chambers et al. (2015) suggested that there is ample evidence that sea-level rise is changing Everglades coastal ecology.

Generally, it is complicated and difficult to predict or anticipate when a landscape transition will occur. However, observing the variability of a system and processes acting upon it over time can suggest whether or not a regime shift is impending (Carpenter and Brock, 2006). Landscape transitions can be anticipated in advance in order to prevent drastic consequences. In the case of the Everglades and other similar wetlands, a regime shift could lead to losses in water quality, damages to diverse habitats, and reductions in vegetation and other natural features (Carpenter and Brock, 2006). Another study noted that an increase in the variance of hydrologic processes over temporal scales may signal a shift in a natural system (Kleinen et al., 2003). It is observed that changes in asymmetry, primarily skewness, can also be a generic indicator of an incoming regime shift (Guttal et al., 2008). These studies have suggested that the higher order statistics (such as variance and skewness) can shed more light on the changing dynamics of these ecological systems. Such analysis can be applied to various hydrologic processes (e.g. precipitation, groundwater elevation, streamflow) that are prominent in the Everglades and can be used to understand, in particular, quantifying their change that can affect the complexity and the dynamics of an ecosystem, not only temporally, but spatially as well.

## 1.1 Study Area

The study area for this investigation is focused on the Everglades region. Located in the southern portion of state of Florida, the Everglades consists of tropical wetlands and serves as a habitat for many diverse wildlife. Forming part of a large drainage basin, the Everglades discharges water southward into the Florida Bay. The Everglades landscape consists of many ridges and sloughs that are connected to local water bodies, promoting connectivity (Larsen et al., 2012). In addition, The Everglades provide services to people by improving the quality of water through natural filtration processes. However, due to the increase in human urbanization and activities, the Everglades ecosystem has been modified drastically. Coupled with climatic changes, the Everglades has been exposed to uncharacteristic forcings. Recently, there is a great interest in observing if there are significant processes that are adversely impacting the ecosystem.

In order to see if there are significant differences within the Everglades region, the area has been classified into three (3) categories, or sub-regions: urban (U), transition (T), and forested (F) sub-regions. The urban sub-region consists of the cities that border the Everglades. For the most part, the area along the east coast of Florida, from Palm Beach to Miami, is designated as urban as well as areas along the west coast of Florida, such as Naples and Cape Coral. The areas where the urban cities meet the Everglades are designated as the transition sub-region. Lastly, the forested sub-region consists of all the vast, natural land within the Everglades. The study area is shown in Figure 1. Note that these areas (e.g., shown in Figure 1) are selected based on the availability of long-term hydrologic data.

In this study, the assessment will focus on understanding and quantifying hydrologic and geomorphic signatures of climatic and anthropogenic changes on the Everglades landscape.



Specifically, hydrologic processes such as rainfall, groundwater elevation, and streamflow will be analyzed to observe their characteristics and how they change over time. The paper is structured as follows: Chapter 2 discusses the review of work done regarding the Everglades. In Chapter 3, a brief description of the data collected and methodology is given. Chapter 4 presents the results and discussion. Summary and conclusions drawn along with broader impacts for future applications are presented in Chapter 5.

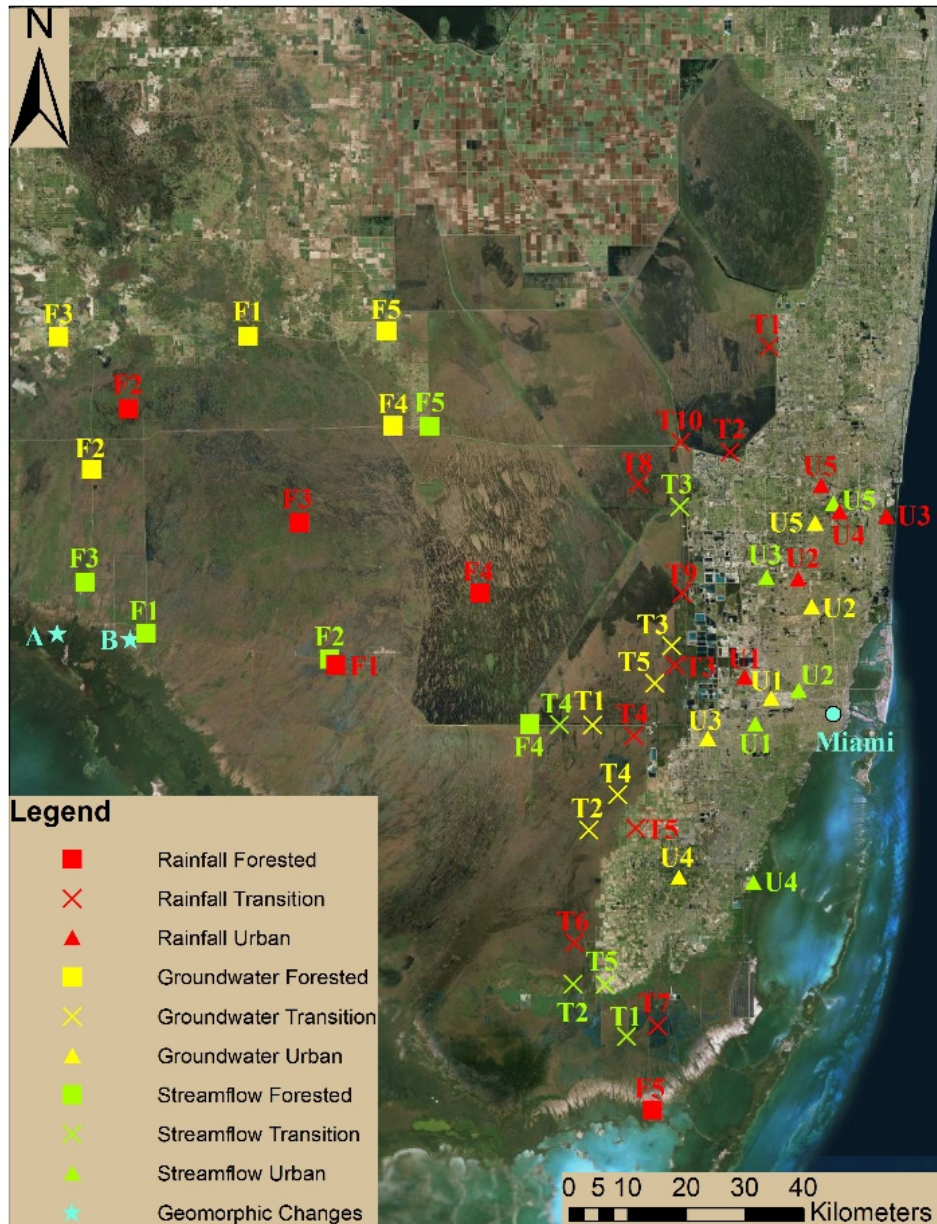


**Figure 1 – Locations of the different USGS stations used in this study along with their notations. From the figure, squares represent stations in the forested area. X's denote stations in the transition area, and triangles denote stations in the urban area. The sample locations depicted as light blue stars denote where the Everglades experienced minor geomorphic changes over time.**

## CHAPTER 2: LITERATURE REVIEW

Many factors influenced how the extent of the Everglades was shaped. The three main factors are: surface water depths, surface and subsurface flow, and phosphorous supply. Recent and historic drivers shaped the Everglades landscape into distinct physical features, such as patterns of ridges, sloughs, and tree islands (Larsen et al., 2011). These mentioned patterns have created dynamic equilibrium in the Everglades for around millennia. In the past century however, human manipulation of the Everglades has also caused a shift in the landscape of the Everglades. Over time, physical features of the Everglades wetlands get diminished which may have detrimental effects on the ecosystem overall. With the ongoing manipulation, it is crucial to restore the Everglades back to its original, natural landscape (Larsen et al., 2011). Observing hydrologic processes and assessing the degree of changes and impacts over time can provide an indicator as to how the landscape is responding to these changes and the effects of those changes to living systems. In essence, the consequences of these changes carry broader impacts that need to be addressed.

Historically, it has been observed that sediments typically are transported from low sloughs to higher ridges. This process provides the formation (shaping) and maintenance of the Everglades landscape (Noe et al., 2009). Certain biological processes take place within the ridges, sloughs, and tree islands that influence how the landscape is shaped. However, should excess stress occur, the landscape may become unstable. In turn, the landscape becomes homogenous, and disrupts existing diverse species (Larsen et al., 2011). For instance, the lack of understanding on how to preserve the mechanisms responsible for the landscape of the Everglades has led to an

altercation of the entire region. This prompted the passing of a comprehensive restoration plan that aims to restore the wetlands back to its original conditions (Larsen et al., 2011).

### 2.1 Sediment Transport and Nutrient Concentration Observations

The primary function of wetlands is to retain sediments from ongoing water flow. Ridges generally experience higher sediment deposition rates while sloughs experience higher sediment entrainment rates, providing a natural balance on the landscape (Noe et al., 2009). There are various factors that control the degree of sediment transport, namely, vegetation, wind, water flow, as well as thermal stratification of water bodies in the Everglades region. (Noe et al., 2009). The variations in the concentrations of certain nutrients, such as phosphorous play a part in how the surface and subsurface flow shape the interior land around it (Larsen et al., 2011). Over time, human activity and climate change has caused additional redistribution of sediments along ridges and sloughs that alters the ridge and slough topography of the Everglades, and it has been a concern to recreate the ideal pre-drainage conditions of the Everglades (Noe et al., 2009). The redistribution of phosphorous as a result of these dynamic changes is a feature worth understanding. Phosphorous removal is necessary in protecting aquatic ecosystems (Noe et al., 2009).

Upon sampling the Water Conservation Area 3A (WCA-3A) region in the Everglades, differences in concentrations and sediment characteristics in ridges and sloughs were very minimal (Noe et al., 2009). The region sampled was an accurate depiction of the original pre-drainage ridge and slough patterns and characteristics of the Everglades. The minimal

differences may be attributed to temporal variations, or a combination of low sediment content, small particle sizes, and low water velocities (Noe et al., 2009).

However, concentrations of phosphorous, sediment fluxes and nutrients differed, in which the ridge experienced increased phosphorous content while the slough saw increases in sediment fluxes. (Noe et al., 2009). For the most part, others have also reported no significant differences in sediment characteristics throughout the Everglades site. However, there are a few instances where sediments characteristics were significantly altered (Noe et al., 2009).

Interestingly, when Hurricane Wilma passed over the Everglades site in late 2005, there was an increase in sediment deposition and concentration (Noe et al., 2009). The deposition occurred mainly in the estuarine mangroves, while an increase in nitrogen concentrations was observed in WCA-3A (Noe et al., 2009). Otherwise, when taking into account the wind, sediment particle sizes, and water velocities, significant transport of sediments and potential nutrients rarely occur (Noe et al., 2009). These are just a few instances where the Everglades landscape experiences geomorphic changes. However, not only does sediment transport affect the topography and landscape dynamics, the area is subjected to coastal effects as well, since the wetlands are situated along the coast of the Gulf of Mexico and the Atlantic Ocean.

## 2.2 Effects of Sea Level Rise and Nitrogen Loading on Coastal Wetlands

Regarding coastal wetlands, there has been concern over the rise in sea levels and its accompanying consequences. As with the increase in nitrogen loading, it is critical that there is a clear understanding of how these events may affect the ecosystem (Larsen et al., 2010). Certain

factors affect the removal of nitrogen from the coastal wetlands. These include soil accretion rate, marsh landscape, surface and subsurface flow, and biological communities (Larsen et al., 2010).

Sea level rise (SLR) is known to affect surface water characteristics such as water levels, hydraulic head, flow velocities, turbulence intensities and bed shear stresses. Consequently, increases of bed shear stresses can lead to an increase in sediment entrainment. Additionally, higher sea levels can inundate coastal tidal marshes, which increase the risk of inland erosion.

Notably, in salt water regions of wetlands, nitrogen removal is reduced due to the interaction between nitrogen and bacteria. As such, more nitrogen will be retained in these areas. Furthermore, the reduction of groundwater discharge due to the increase in sea level rise also prevents the removal of nitrogen (Larsen et al., 2010). In freshwater marshes, the increase in nitrogen loading leads to bacterial immobilization, effectively reducing the nitrogen removal. However, an increase in the exchange between surface flow and tidal creeks may promote the increase in nitrogen removal (Larsen et al., 2010). On the topic of surface flow, various parameters, such as local topography, geology, and land use/land cover can influence the natural pattern of surface flow. Thus, investigating the surface flow process as a function of these parameters may improve our understanding of their changing signatures on the wetlands.

### 2.3 Vegetation Characteristics

Vegetation communities and sediment transport are crucial in not only maintaining the landscape, but also sustaining diverse biological life (Larsen and Harvey, 2010). Vegetation communities existing underwater (sloughs) also influence how river flow affects the landscape. Where there is an increase in vegetation communities, the subsurface flow tends to be resisted by

the individual stems of the plants, hindering the effects of shaping or eroding of the landscape. In essence, vegetation communities provide feedback that dominates the lateral aspects of the landscape. Similarly, differential peat accretion feedbacks govern the longitudinal features of the landscape (Larsen et al., 2011). Sediment redistribution from sloughs to ridges is possible once flows exceed entrainment thresholds. However, finer particles are not affected by flow, since existing vegetation may be responsible for intercepting a decent number of fine sediments (Larsen et al., 2011).

Moreover, the higher the water depth is, the higher the resistance caused by the vegetation communities and minor nutrient concentrations (Larsen et al., 2011). Water surface slope also determines the extent of landscape evolution. The steeper the surface slope, the more potential the surface flow has in shaping (widening) the exteriors of ridges, and sloughs (Larsen et al., 2011). Vegetation allows for resistance in subsurface flow, preventing disturbances. However, when the ecosystem is susceptible to significant changes in surface flow, the channel beds may experience great shifts, altering the state of the landscape pattern (Larsen and Harvey, 2010). With the presence of emergent vegetation, the effects of bed shear stresses are reduced (Larsen et al., 2010).

Vegetation communities influence flow regimes. As a result, the change in the flow regimes affects how erosion and deposition processes occur in aquatic ecosystems (Larsen et al., 2009). However, understanding the effects of vegetation on bed shear stress can provide additional information about the evolving ridge and slough landscape. It can also provide insight as to why the landscape is becoming more homogenous (Larsen et al., 2009). In the Everglades for instance, vegetation communities exhibited a dominant effect of reducing bed shear stresses,

which reduced sediment entrainment. It was also observed that water surface slope also tends to reduce bed shear stresses. Based on these results, management organizations can focus on what measures to take in order to restore heterogeneity and the original ridge/slough landscape of the Everglades (Larsen et al., 2009). A basic understanding of how landscapes respond to adverse changes and provide feedback is necessary.

#### 2.4 Landscape Feedbacks and Connectivity

Landscapes exhibit feedbacks that indicate how the landscape changes over time. Feedbacks at a small scale (local facilitation), argue that living systems (i.e. organisms) adjust their surroundings so that any feedback is positive (Larsen and Harvey, 2010). The scale is no longer local once it surpasses a spatial threshold. In this case, feedbacks that occur in this region are negative, which explains why organisms thrive in small scales (Larsen and Harvey, 2010).

Wetlands that follow the ridge/slough landscape pattern, such as the Everglades, have unique but valuable ecosystem functions that should be preserved (Larsen and Harvey, 2010). Wetlands exhibit scale-dependent feedbacks which involves nutrient accumulation. These feedbacks over time are responsible for shaping distinct wetlands with distinct patterns (Larsen and Harvey, 2010). The Everglades exhibits a vegetative pattern that has been stable for millennia. In the past century, human activity modified the vegetation patterns, which in turn caused topographic changes and land cover (Larsen and Harvey, 2010). Understanding these feedbacks and the dynamics of landscape evolution can help restore modified landscapes to their original conditions (Larsen and Harvey, 2010).



Feedbacks can come in several forms, for example, sediment transport feedback and differential peat accretion feedback. Feedbacks can interact with each other and shape a certain landscape in a unique way. The extent of how feedbacks regulate landscape varies among wetlands worldwide (Larsen and Harvey, 2010). For instance, in the vegetative scale, the feedbacks mentioned can promote vegetative emergence. In the landscape scale, these feedbacks can regulate how open channels are modified (Larsen and Harvey, 2010).

Establishing a relationship between hydrologic and ecologic conditions of certain areas of the Everglades can help provide a better understanding of how sediment transport takes place. More importantly, this relationship can help send warning signs of potential degradation or difficulties in restoration efforts in advance (Larsen et al., 2012). The extent of sediment transport can also affect biodiversity. The fact that there has been a decline in biodiversity emphasizes the need for restoration (Larsen et al., 2012).

Connectivity is defined as the degree in which a landscape facilitates or impedes movement along a path. Different forms of connectivity exist. For instance, structural connectivity describes the physical adjacency of landscape features. Additionally, function connectivity focuses on how processes such as water flow exhibits landscape adjacency. The theory of connectivity can be used to explain how wetlands respond to hydrologic events at large scales. Connectivity benefits ecology by governing the distribution of habitats over time (Larsen et al., 2012).

In a case study, a process used to analyze the relationship between hydrologic and ecologic conditions was a directional connectivity index (DCI) graphic analysis. Complied of images with a set resolution, any changes in image rotations may indicate separation of

hydrologic and ecologic conditions of the Everglades, which is a sign of potential degradation. In the case of the Everglades, the DCI showed that connectivity among sloughs deteriorated quickly. This may suggest that the landscape is becoming more homogenous with the increase in the growth of sawgrass. (Larsen et al., 2012).

Longitudinal patterned wetlands are subject to drastic shifts. Any remaining intact portion of a wetland consisting of its unique pattern can and needs be preserved (Larsen and Harvey, 2010). Natural, yet sufficient, water flows and levels are required to maintain the wetland's original landscape. By recognizing these drastic landscape shifts, it is necessary to create new best management practices in order to anticipate these changes ahead of time and prevent them from occurring (Larsen and Harvey, 2010). Investigating the dominant hydrologic processes in depth can provide additional insight as to how their variations can be quantified.

### 2.5 Quantifying Groundwater Variations

Quantifying the variations of groundwater levels and recognizing their implications on dynamic landscapes (i.e., wetlands) is essential. Hydrologic processes, for example, can affect the complexity and dynamics of groundwater flow fields, not only temporally, but spatially as well. These hydrologic processes are driven by climate change. With the increasing effects of climate change occurring over the past decades, evidently, the behavior of groundwater systems is more distinct than usual. Geologic characteristics can also affect the response of groundwater systems (Winter, 1999). Along with climate change, the increase in urban development impacts the groundwater systems as well.

According to the Intergovernmental Panel on Climate Change (IPCC), human activities continue to alter the atmosphere and contribute towards the emission of greenhouse gases (IPCC, 2001). Eckhardt and Ulbrich (2003) observed the changes of rainfall on groundwater recharge over different climate scenarios in western Germany. For one scenario, an increase in CO<sub>2</sub> concentrations coupled with minor climate change resulted in groundwater recharge reductions of 3%. Another scenario, consisting of a larger increase in CO<sub>2</sub> concentrations coupled with more significant climate changes resulted in a groundwater recharge reductions of 7.5% (Eckhardt and Ulbrich, 2003). Although this study focuses on a low mountain range in Europe, this type of analysis can be applied to other natural features, such as wetlands.

For the Everglades ecosystem, this is an ongoing concern that needs to be addressed. However, groundwater flow is not the only process influenced by rapid urban development. Streamflow is another major hydrologic process that gets impacted by urbanization. As a result, natural basins are disrupted, and flow patterns are out of equilibrium. Observing these signatures in hydrologic processes can serve as an indicator as to what extent is climate change impacting the wetlands.

### 2.6 Streamflow Alterations

Observing changes in major river basins over a period of time can serve as an indicator for climate change. Specifically, in another case study, analyzing the streamflow records in Minnesota's major basins reveals that streamflow trends are periodic and are on the order of 13-25 years roughly. Furthermore, there is amplification in the data in recent years (Novotny and Stefan, 2006). What this implies is that with climate change, the risk of intense events increase

and along with that, the risk of flooding rises. Beyond that, increased amounts of mean streamflow could lead to improved water quality and a better habitat for aquatic ecosystems (Novotny and Stefan, 2006). Of course, what occurs in one region will differ in another. Perhaps the streamflow change in wetland areas may have different implications. With an ecosystem like the Everglades that has been subject to many perturbations, it's critical for water management entities to understand hydrologic changes (mainly in rainfall, groundwater levels, and streamflow) and better protect/restore the natural features of the landscape.

### CHAPTER 3: METHODOLOGY

To quantify the ongoing effects of climate change on the Everglades, the study focuses on three (3) hydrologic processes for each sub region. These processes are: (1) rainfall,  $R(t)$ ; (2) groundwater elevation,  $G(t)$ ; and (3) streamflow,  $Q(t)$ . Historical data for groundwater elevation and streamflow processes are available at the United States Geological Survey (USGS) database, the South Florida Water Management District (SFWMD), and the Everglades National Park (ENP). The data for rainfall are obtained from the Everglades Depth Estimation Network (EDEN) within the USGS database as well as SFWMD.

Groundwater elevation data were obtained from five USGS stations for each sub region. Note that the south Florida area is situated above the Floridan aquifer, which is a major source for providing fresh, drinking water to major urban cities and also used for the Everglades' ecosystem restoration and for the most part, this aquifer is thinly confined. As for rainfall, five gauges for the urban and forested sub-regions were obtained whereas for the transition sub-region, ten locations were chosen. For streamflow, five stations were obtained for each sub-region. These data were carefully observed and treated for errors (e.g. instrumental, missing gaps) and considered such that the data had roughly the same time periods depending on data availability. The locations of these stations are displayed in Figure 1. Table 1 lists the data gauges along with their time ranges and properties.

Before analyzing the data, the data was processed in order to ensure that the analysis could be carried out in the best possible manner. In some cases, the raw data collected contained missing values, which may give rise to uncertainty. On average, the percentage of missing data for  $R(t)$ ,  $G(t)$ , and  $Q(t)$  are 2.07%, 2.79%, and 1.05%, respectively. For the time series analysis, it

is preferred that the data sets are continuous. In an attempt to reduce the uncertainty and adjust the raw data, a cubic interpolation process was used to interpolate any gaps in the data based on the existing values before and after the gap, resulting in a continuous time-series for the study time period. In the case for streamflow, a few gauges contained negative values and were removed as a part of data treatment and the resulting gaps were filled with the above discussed cubic interpolation.

The digital elevation models (DEM) were obtained from the ASTER Global DEM database. According to the USGS EarthExplorer site, which contains the same DEMs from the ASTER database, these images were processed around 2011. The resolution of the DEMs was 30 m, or about 1 arc-second. Figure 2 shows the sampled locations from the study that corresponds to the extracted river network. Basin properties will be extracted from watersheds and compared across the sub-regions to assess any differences and explain what contributes to these changes.

From the hydrologic data collected, their histograms will be computed and compared across sub-regions. The statistical properties of these histograms will be obtained in order to further assess the variability and shape characteristics (i.e. signatures) that these processes consist of. This will be done by implementing a differencing approach. Next, spectral analysis is used to analyze the degree of variability across time scales. Quantifying the degree of asymmetry can provide information on whether or not the wetlands are experiencing major stresses and shifts, which may lead to landscape transitions.

The inter-arrival times of extreme events (>95%) will be computed to observe the power-law regimes that govern the hydrologic events. Any differences in the power-law regimes across the wetlands may further suggest anthropogenic and climatic influence on the Everglades.

Reviewing the higher-order statistics of these hydrologic data may reveal their distinct signatures and the implications that are present due to the ongoing effects of human activities and climate.

**Table 1 – Gauges and their properties used in this study.**

Hydrologic process	Sub-region	Station ID	Time range	Data length (years)	Minimum	Maximum	Mean	Variance	Standard deviation
Rainfall (cm)	Urban	U1 - MIAMI_FS_R (WMD)	1991-2014	24	0	33.71	0.48	1.76	1.33
		U2 - S29Z_R (WMD)	1991-2016	26	0	24.87	0.42	1.41	1.19
		U3 - HOLLYWOOD (WMD)	1991-2014	24	0	33.99	0.46	2.01	1.42
		U4 - S13_R (WMD)	1991-2014	24	0	24.13	0.41	1.45	1.20
		U5 - FT. LAUD_R (WMD)	1971-2016	46	0	22.83	0.79	2.58	1.61
	Transition	T1 - SITE_19 (EDEN)	2002-2014	13	0	14.96	0.36	0.98	0.99
		T2 - SITE_99 (EDEN)	2002-2014	13	0	9.27	0.35	0.78	0.88
		T3 - G-3818 (EDEN)	2002-2014	13	0	12.65	0.37	0.92	0.96
		T4 - G-3576 (EDEN)	2002-2014	13	0	12.83	0.38	0.97	0.99
		T5 - G-3626 (EDEN)	2002-2014	13	0	16.48	0.40	1.14	1.07
		T6 - NTS10 (EDEN)	2002-2014	13	0	13.34	0.36	0.93	0.96
		T7 - EVER8 (EDEN)	2002-2014	13	0	13.31	0.33	0.91	0.96
		T8 - EDEN_4 (EDEN)	2002-2014	13	0	13.46	0.34	0.87	0.93
		T9 - S31_H (EDEN)	2002-2014	13	0	11.35	0.34	0.82	0.90
		T10 - S34_H (EDEN)	2002-2014	13	0	10.21	0.34	0.84	0.92
	Forested	F1 - Tamiami_Canal_40_Mile_Bend_to_Monroe (EDEN)	2002-2014	13	0	10.21	0.35	0.86	0.93
		F2 - BCA2 (EDEN)	2002-2014	13	0	10.01	0.38	0.90	0.95
		F3 - BCA15 (EDEN)	2002-2014	13	0	10.13	0.36	0.83	0.91
		F4 - W11 (EDEN)	2002-2014	13	0	12.27	0.34	0.87	0.93
		F5 - Stillwater_Creek (EDEN)	2002-2014	13	0	18.49	0.28	0.85	0.92
Groundwater elevation (m)	Urban	U1 - G-3329 (USGS)	1984-2015	32	0.41	2.40	0.84	0.02	0.14
		U2 - S-18 (USGS)	1973-2014	42	0.31	2.18	0.64	0.01	0.12
		U3 - G-3572 (USGS)	1994-2014	21	0.45	2.59	1.08	0.03	0.17
		U4 - G-614 (USGS)	1973-2015	43	-0.17	3.43	0.98	0.08	0.28
		U5 - G-1223 (USGS)	1973-2015	43	0.32	1.97	0.75	0.03	0.19
	Transition	T1 - G-618 (USGS)	1973-2014	42	0.96	2.67	2.04	0.05	0.22
		T2 - G-1502 (USGS)	1973-2015	43	0.16	2.51	1.79	0.14	0.38
		T3 - G-975 (USGS)	1958-2015	58	0.64	2.61	1.73	0.09	0.30
		T4 - G-3272 (USGS)	1995-2015	21	0.64	2.57	1.92	0.09	0.30
		T5 - G-1488 (USGS)	1970-2015	46	0.84	2.54	1.89	0.06	0.25
	Forested	F1 - HE-1063 (USGS)	2003-2014	12	3.51	5.84	5.07	0.22	0.47
		F2 - C-296 (USGS)	1997-2014	18	2.20	3.98	3.40	0.12	0.35
		F3 - C-503 (USGS)	1996-2015	20	3.76	6.00	4.97	0.15	0.38
		F4 - C-54 (USGS)	1973-2014	42	2.41	4.20	3.33	0.07	0.27
		F5 - HE-862 (USGS)	1988-2015	28	1.78	4.54	3.69	0.18	0.42
Streamflow (cms)	Urban	U1 - 02289500 (USGS)	1959-2015	57	0	31.70	4.33	8.20	2.86
		U2 - C6.NW36 (USGS)	1959-2011	53	0	48.96	6.23	45.15	6.72
		U3 - C9.NW67 (USGS)	1962-2011	50	0	43.87	6.66	31.33	5.60
		U4 - S21_S (WMD)	1978-2014	37	0	73.44	5.12	49.35	7.03
		U5 - S13 (WMD)	1978-2012	35	0	27.51	3.98	13.35	3.65
	Transition	T1 - 02290769 (USGS)	1968-2015	48	0	83.20	5.12	71.81	8.47
		T2 - NP-TSB (ENP)	1960-2016	57	0	27.56	1.61	7.82	2.80
		T3 - S9_P (WMD)	1957-2016	60	0	68.88	5.41	68.77	8.29
		T4 - L29 (USGS)	1963-2013	51	0	50.37	4.79	37.74	6.14
		T5 - S177_S (WMD)	1983-2012	30	0	49.97	4.91	52.55	7.25
	Forested	F1 - 02288800 (USGS)	1960-2015	56	0	170.08	12.00	358.22	18.93
		F2 - 02288900 (USGS)	1963-2015	53	0	205.74	11.40	291.28	17.07
		F3 - 02291000 (USGS)	1952-2014	63	0	8.26	2.30	3.50	1.87
		F4 - S333 (WMD)	1978-2016	39	0	69.34	6.62	71.84	8.48
		F5 - S140-TOT (WMD)	1969-2016	48	0	60.36	4.31	41.88	6.47



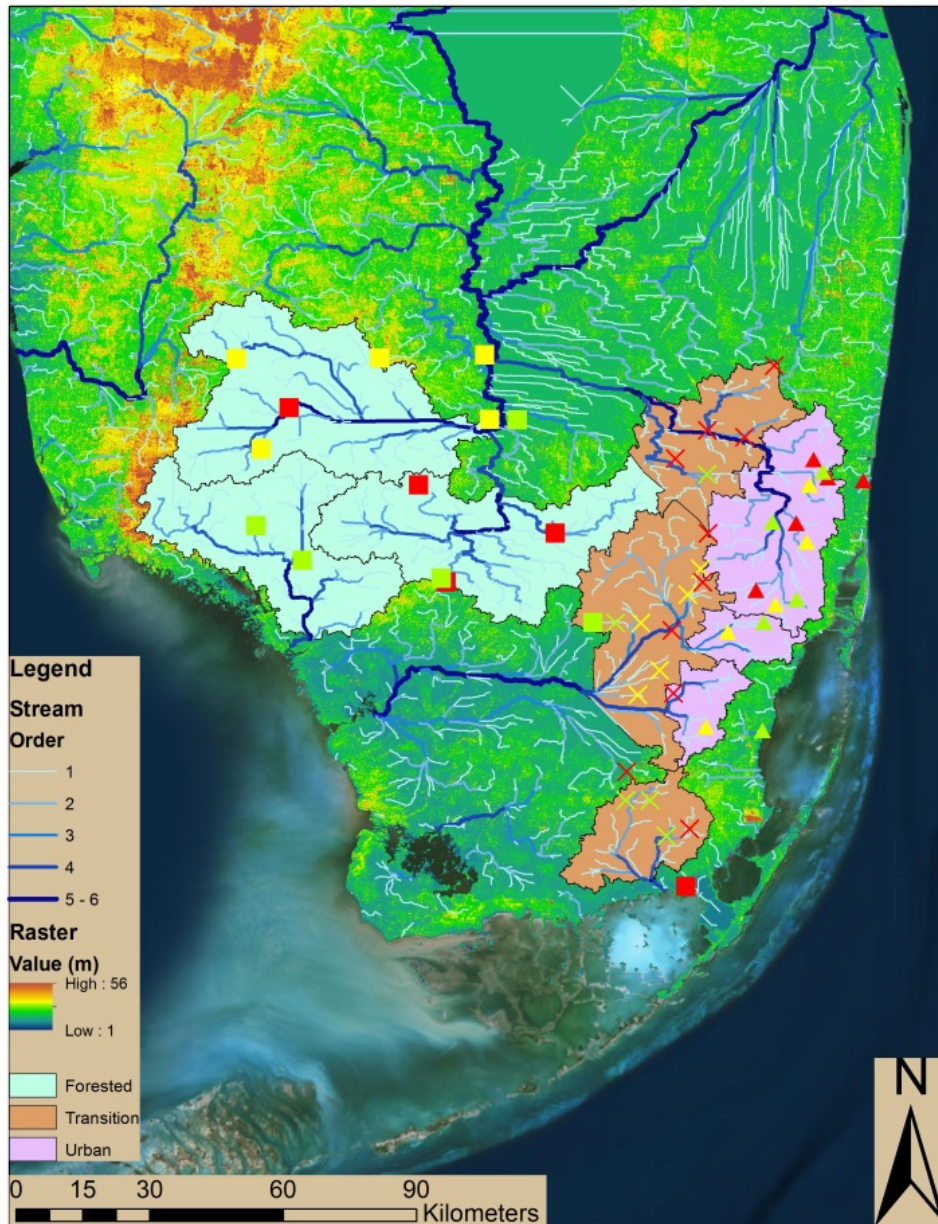


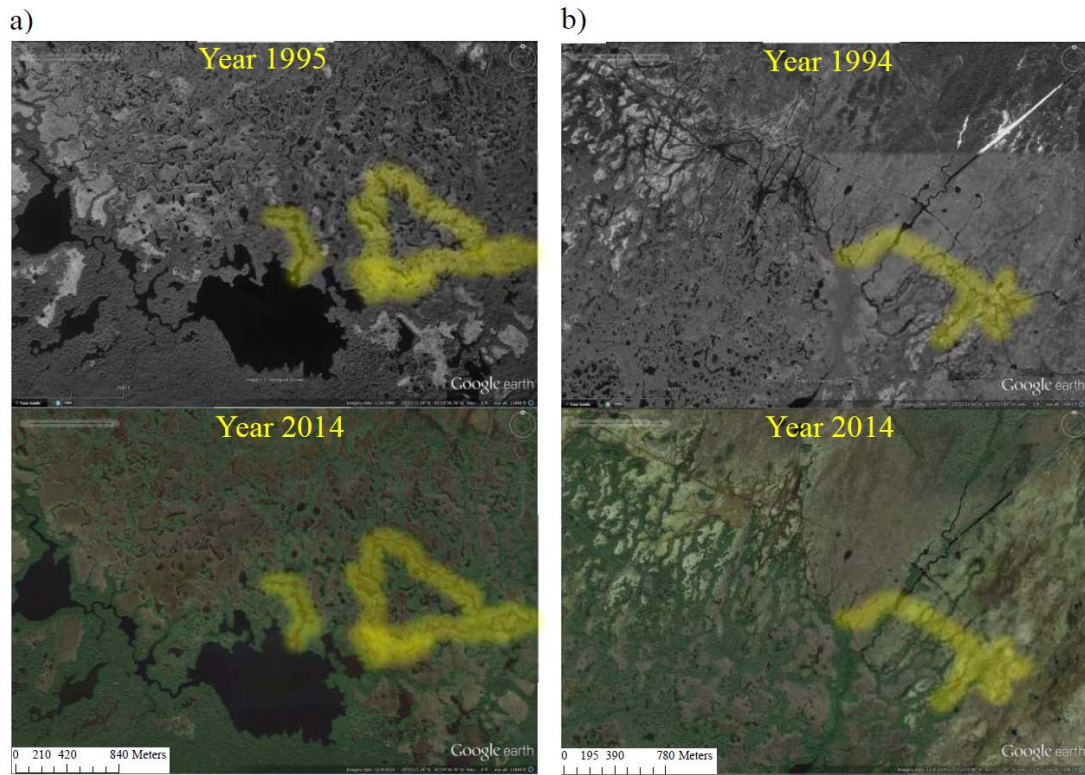
**Figure 2 – Stream network in south Florida. Also, three sample watersheds for the urban, transition, and forested sub-regions are mapped out.**

## CHAPTER 4: RESULTS AND DISCUSSION

In order to quantify changes in the Everglades' wetland environment over time, a clear understanding of how hydrological processes change, is necessary. These changes in the hydrologic processes can be driven by climate change as well as by human intervention, such as urban development, groundwater pumping, and construction of canals. With the increase in urban development, especially near the Everglades, there is a greater interest in understanding how hydrologic systems, particularly groundwater flow patterns, within wetland ecosystems are affected under developed conditions (Sophocleous, 2002). Additionally, observing and characterizing the changes in major river basins' hydrology and geomorphology over a period of time can serve as an indicator for climate change (Novotny and Stefan, 2006). The development and operation of canals effectively redirects local streams from their original path, altering the natural flow pattern and causing the Everglades wetlands and wildlife systems to respond to this sudden change. This prompts additional understanding of how hydrologic systems are being carried out.

To observe the geomorphic changes in the Everglades region over time, current satellite images are compared to historical satellite images of the region. Using the Google Earth historical time slider feature, the historical images of the Everglades date back to 1994-1995, while the current images are as recent as December 2014 (the last available month when the analysis was started). Comparing these two sets of images, it can be seen that the changes in the geomorphology of the Everglades region occur in localized areas, (Figure 3). These geomorphic changes observed in the Everglades consist of changes in the shapes and sizes of natural channels and water bodies.

Figure 3 shows the satellite images for two regions at two different time instants. As can be seen from this figure (highlighted in yellow), significant changes occurred on the landscape. For example, in Figure 3a (comparing the top and bottom panels, see also Figure 3b), the small channel in the center sees minor changes to its geometry. On the right hand side of Figure 3a, there is an addition of small streams in 2014. In Figure 3b, several segments of different channels disappear, while minor tributaries seem to emerge in 2014. These changes in the landscape and equilibrium could result in the propagation and formation (extinction) of new (old) streams and may be due to various changing hydrologic processes under changing climate and anthropogenic forcings that contribute to the accelerated changes in geomorphic features over time. It is likely that even looking back more than 20 years (not performed here due to unavailability of data), the extent of the geomorphology in the Everglades region is greater. To relate these visually observed geomorphic changes to the hydrological processes, one can further quantify the time changes of different variable processes acting on the Everglades.



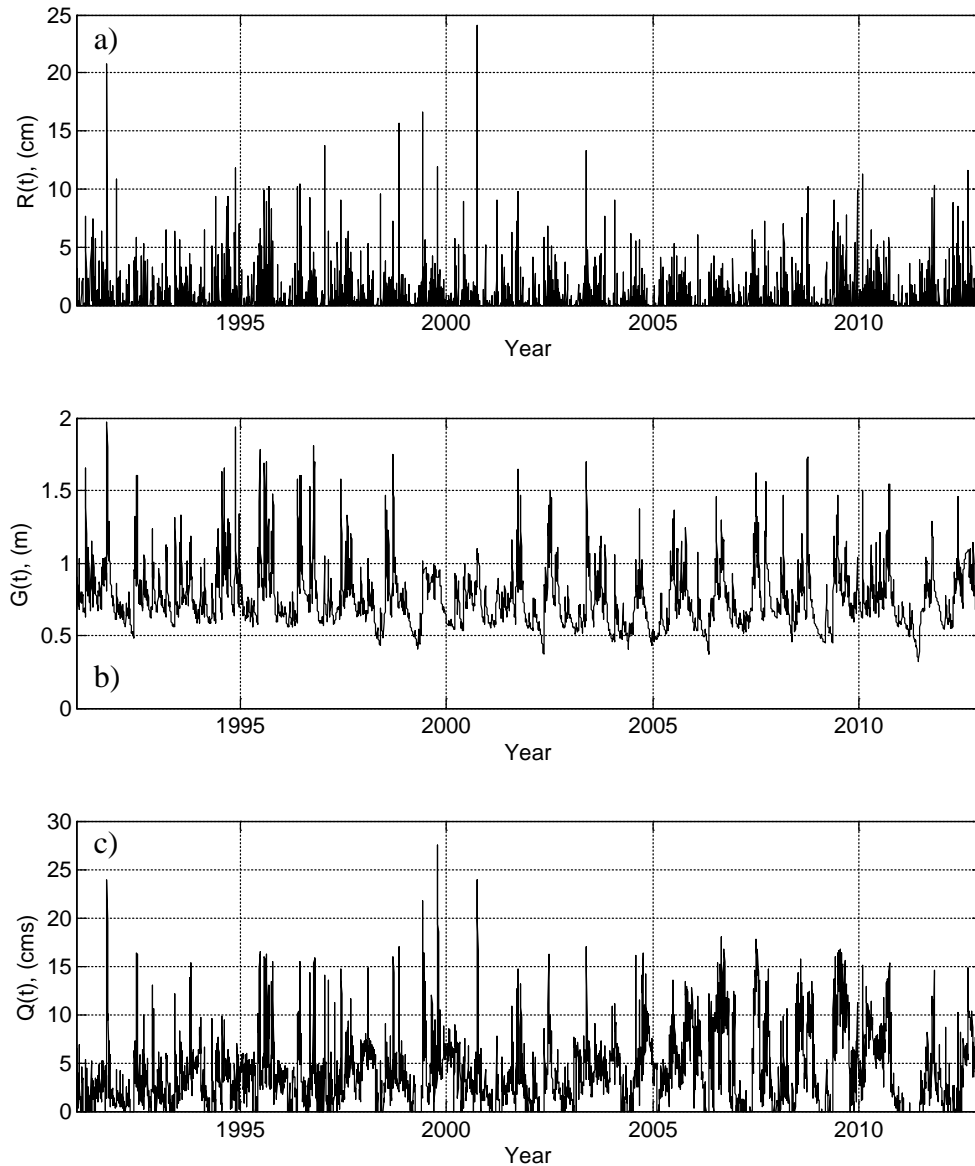
**Figure 3 – Sample local geomorphology of the Everglades for two different locations (shown in right and left panels) and two different instant of times corresponding to years 1994-5 (top panels) and year 2014 (bottom panels). Examples of changes in local geomorphology are highlighted in yellow. For example, in (a) addition of minor streams or water bodies and changes in channel geometry can be seen. In (b) over time, at the highlighted locations, minor streams and other features no longer exist. These images correspond to points A and B, indicated in Figure 1.**

Figure 4 shows the sample time series for rainfall  $R(t)$ , groundwater elevation  $G(t)$ , and streamflow,  $Q(t)$ , collected at the sampling interval of 1 day. As can be seen from this figure, significant variability and trends are observed in the time series plots. For example, both in  $G(t)$  and  $Q(t)$ , a seasonal pattern is observed along with a local increase/decrease in the mean (see, for e.g., a decrease in the mean in  $G(t)$  in Figure 4b between the year 2005 and year 2007). In fact, several locations for both  $G(t)$  and  $Q(t)$  showed changes in the mean and variance over time even in the case of the forested sub-region, suggesting the influence of changing climate on these hydrologic variables (e.g., Figure 5 for various randomly selected location for  $G(t)$  and  $Q(t)$  gauges from the forested sub-region). Additionally, both  $G(t)$  and  $Q(t)$  show periodic/oscillatory behaviors throughout time.

Figure 6 shows the probability distribution functions (PDFs) for each station with respect to the sub-regions for rainfall,  $R(t)$ , (Figure 6a), groundwater elevation,  $G(t)$ , (Figure 6b), and streamflow,  $Q(t)$ , (Figure 6c). The PDFs for rainfall (Figure 6a) in all sub-regions, as expected, appear to behave mostly similar relative to one another suggesting that the rainfall does not change significantly within the study area, regardless of sub-regions.

From Figure 6b, it can be seen that groundwater elevation varies significantly with respect to sub-region. For example, the PDFs for the case of urban groundwater are significantly shifted towards the left as compared to the PDFs of the forested and transition sub-regions; groundwater elevations range from 0-2 m in urban, 1-2.5 m in transition, and 2.5-6 m in the forested sub-regions. In addition to the shifting of the PDF, a visual change in asymmetry is also observed for the three different sub-regions. In particular, in the urban areas, the PDFs are roughly positively skewed, whereas the transition and forested areas have PDFs that are

negatively skewed. This behavior can be explained by the groundwater mechanisms present in South Florida. The Forested area in South Florida is situated at higher elevations (higher hydraulic heads) than the urban areas (Finkl and Charlier, 2003). In terms of groundwater flow, it is natural that the forested areas would contain higher groundwater levels, whereas the urban coasts discharges groundwater, hence the lower groundwater amounts (Finkl and Charlier, 2003). In addition, this behavior could be a result of recent urbanization and increased population densities along the east coast of Florida, which has led to higher groundwater pumping for consumption purposes. As for streamflow (Figure 6c), the histograms behave in a pattern that's roughly similar to rainfall, but more nonlinearly spread out and will be discussed later in more details.



**Figure 4 – Sample time series plots for daily (a) rainfall,  $R(t)$ , (b) groundwater elevation,  $G(t)$ , and (c) streamflow,  $Q(t)$ .  $R(t)$ ,  $G(t)$ , and  $Q(t)$  correspond to stations U4 (red), U5 (yellow), and U5 (green) from Figure 1a respectively. Note that all the time series are shown for similar time periods for visual comparison, however, longer time series exist and were analyzed for  $G(t)$  and  $Q(t)$ . cms in part (c) represents cubic meter per second.**

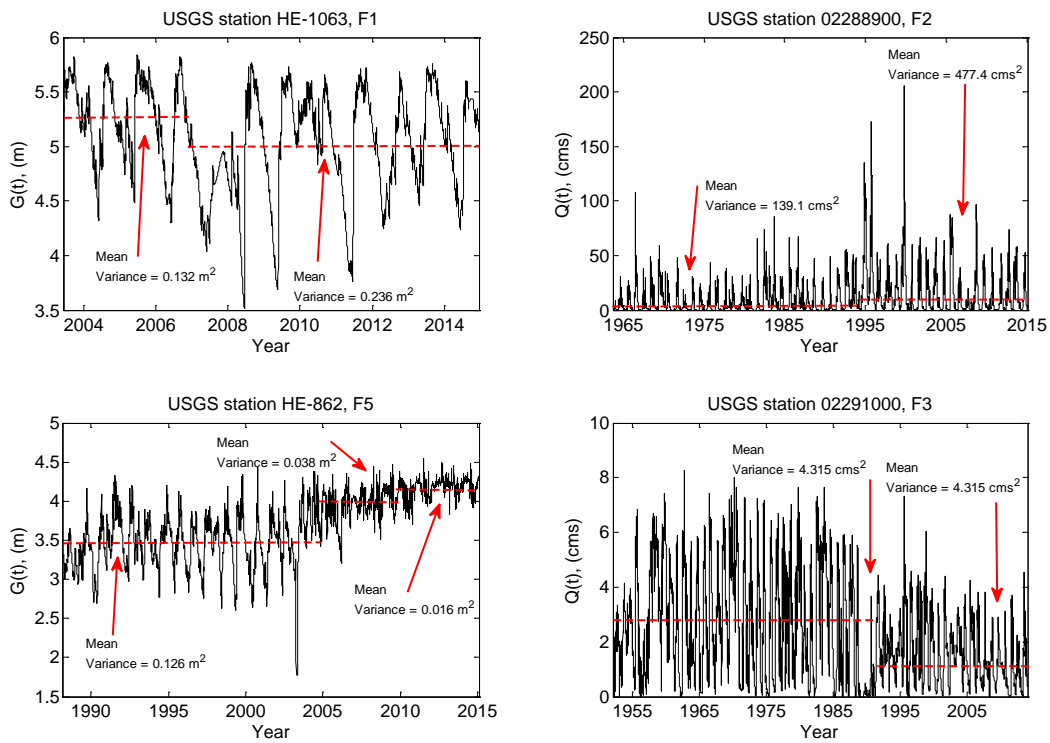


**Figure 5 – Randomly selected locations where groundwater elevation (left column) and streamflow (right column) experience changes in mean and variance in their time series, highlighting effects of climate change. All these gauges are located in the forested sub-region.**



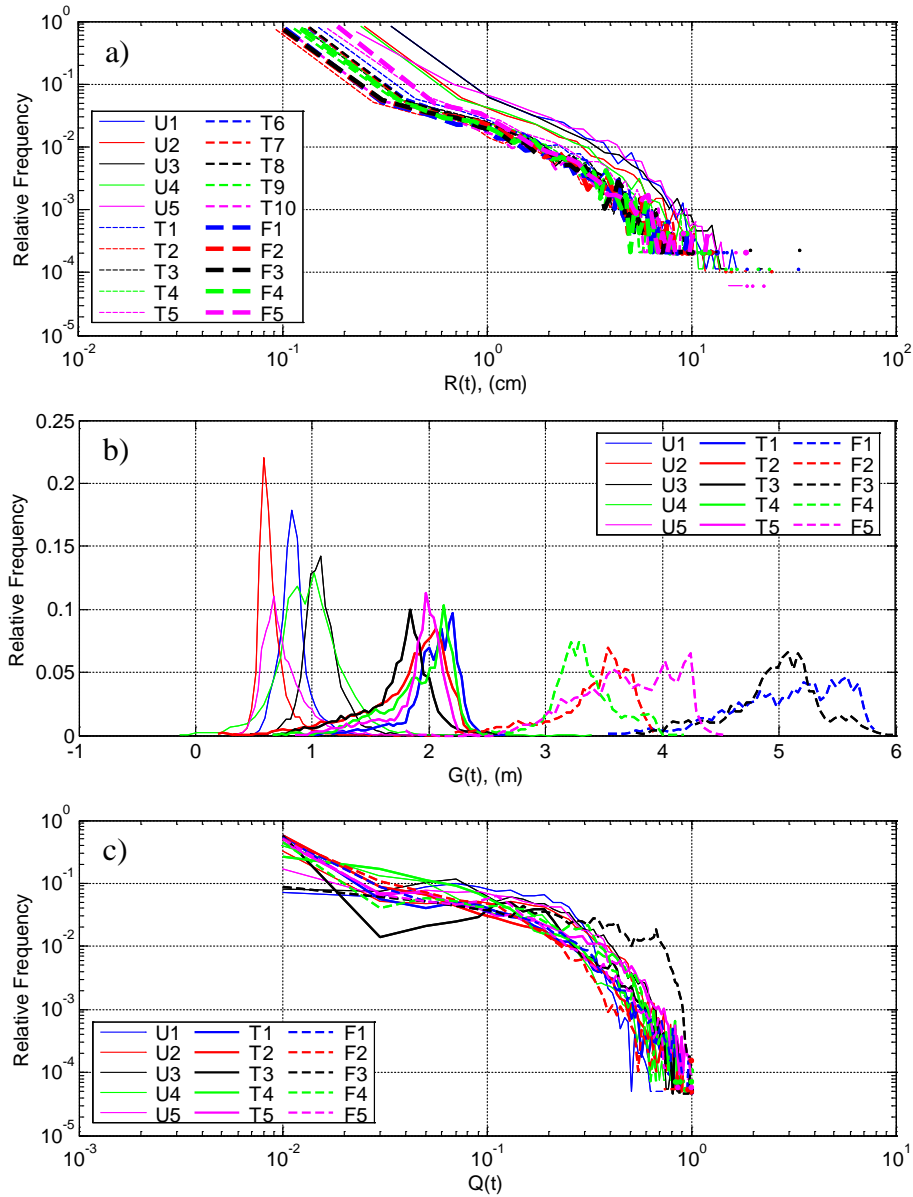


**Figure 6 – Probability density functions (PDFs) for rainfall (a), groundwater elevation (b), and streamflow (c). U, T, and F denote urban, transition, and forested sub-regions, respectively. For streamflow, the PDFs are normalized using  $(Q-Q_{\min})/(Q_{\max}-Q_{\min})$ , since streamflow is a function of basin size.**

To further quantify the asymmetry in the PDFs of  $R(t)$ ,  $G(t)$  and  $Q(t)$ , their increments are computed as a function of time scale, which can be represented as follows:

$$\Delta x(t, a) = \Delta x(t + a) - \Delta x(t) \quad (1)$$

where,  $\Delta x$  is the incremental difference of the time series;  $t$  and  $a$  represent time and lag (scale), respectively. Semi-log PDFs for all three hydrologic processes and their sub-regions are shown in Figure 7 at a time lag,  $a = 1$  day. As seen in Figure 7, all the three processes' increments PDFs show a double-exponential type of behavior. In addition, the PDFs of the increments for groundwater elevation,  $G(t)$ , and streamflow increments,  $Q(t)$ , appear to be asymmetric, whereas the rainfall increments,  $R(t)$ , are just about symmetric (Figure 7a).

To conclude whether the rainfall PDFs in Figure 6a are similar to each other, the quantile-quantile (QQ) plots of their increments (Figure 7a inset) are plotted against each other in order to observe the degree of linearity. Additionally, the Kolmogorov-Smirnov (KS) two-sample test is used to assess the PDFs in each sub-region to see if the sample data are drawn from the same exponential distributions. The test is applied several times since each sub-region had to be paired to another (i.e., urban to transition, urban to forested, and transition to forested). The alternative hypothesis states that the two sample datasets are drawn from different distributions. At a significance level of 5%, the KS test concluded that the sample sets of data are drawn from the same exponential distributions. In other words, the null hypothesis, for all cases, is not rejected. Furthermore, the QQ plots of the rainfall increments plot linearly for all pairing cases, as shown in Figure 8, which reaffirms that the rainfall data come from the same distributions.

The ensemble average PDFs of the increments of  $G(t)$  and  $Q(t)$  are shown as insets of Figures 7b and 7c, respectively (the ensemble average increment PDF for  $R(t)$  is shown as an inset in Figure 7a). As can be seen from these inset PDFs, for the case of  $G(t)$ , the PDFs are highly leptokurtic (high kurtosis) for urban as compared to the forested and transition sub-regions whereas the trend is reversed for  $Q(t)$ , i.e., the forested sub-regions show high kurtosis as compared to urban and transition. For both  $G(t)$  and  $Q(t)$ , the PDFs for the transition sub-region lie between the urban and forested sub-regions. The construction of several canals around the Everglades over time allows the streamflow to bypass the Everglades, which may explain the contrasting streamflow behavior for the case of the urban (lower fluctuations in streamflow in urban areas) and forested sub-regions in the PDFs (i.e., Figures 6, 7) (Chambers et al., 2015).

Figure 9 shows the increment difference PDFs for the hydrologic processes using a lag of 365 days. For this case, these PDFs appear more symmetric for all three processes, compared to Figure 7. The reason for this is due to the natural periodicity of these processes. If one were to measure a process on a given day, and then take another measurement a year later, there is a tendency for those measurements to be very similar, such that the difference between them is nearly zero, hence it has zero degree of asymmetry. Ideally, one can assess the degree of asymmetry as a function of scale, or lag, to see how the increments behave over time.

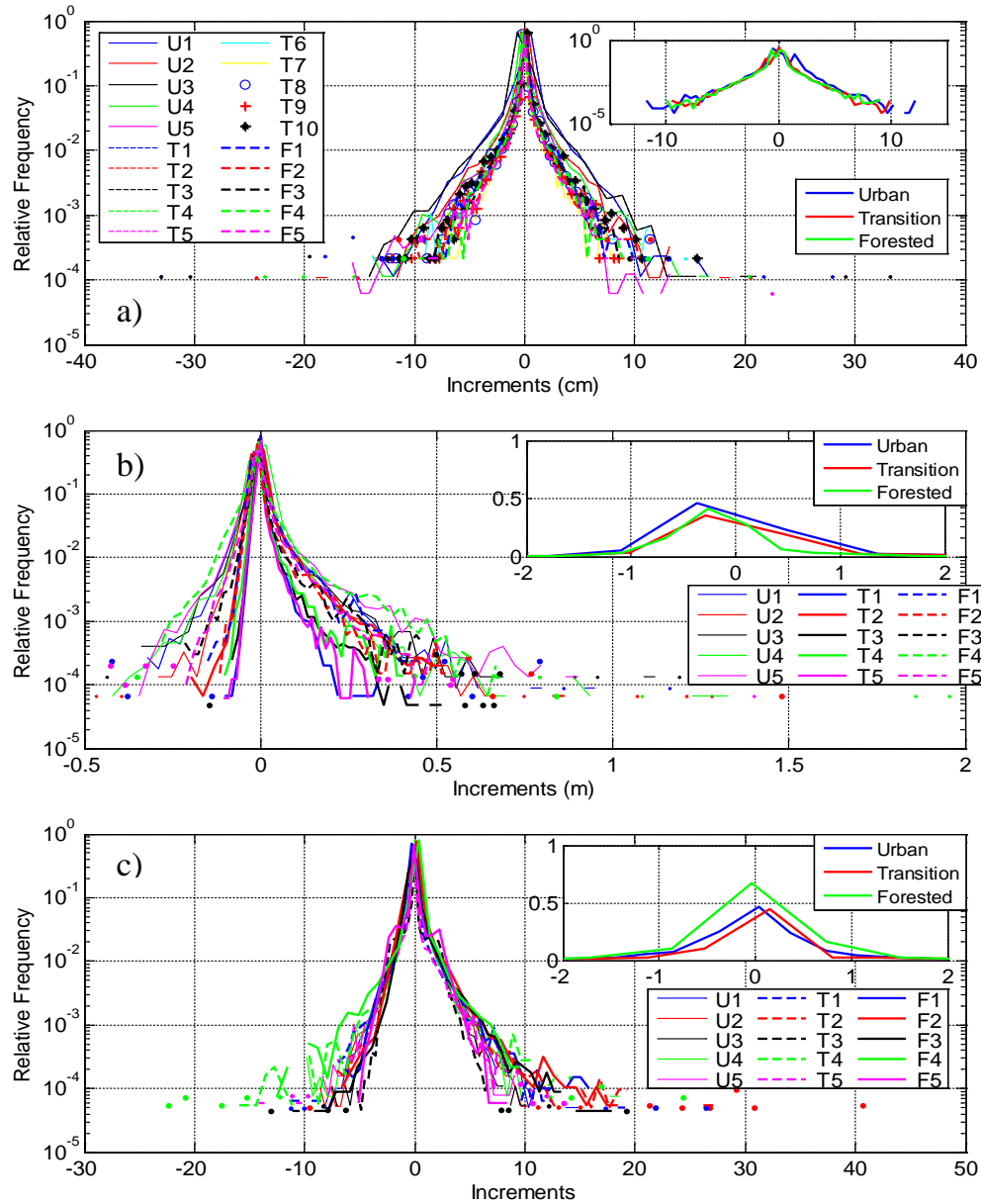


**Figure 7 – PDF increments for rainfall (a), groundwater elevation (b), and streamflow (c). Note the asymmetry in the groundwater elevation and streamflow plots. Rainfall PDFs show symmetric behavior. Also note that these PDFs were computed at a scale of 1 day. The insets show the ensemble averages of the increment PDFs for each sub-region. The x-axes represent standardized increments computed using  $(x-\mu)/\sigma$ .**

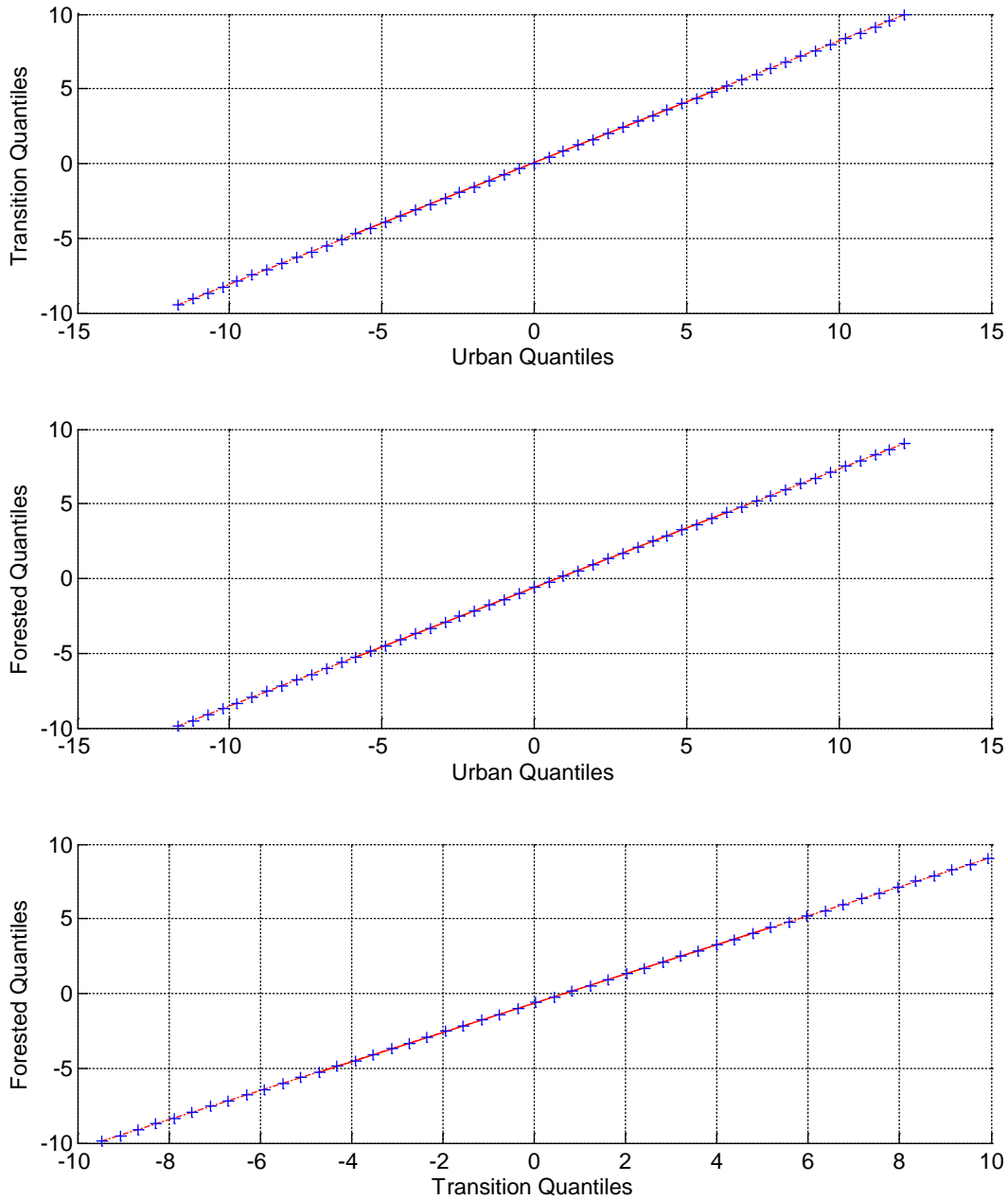


**Figure 8 – Quantile-Quantile (QQ) plots of each sub-region paired to another sub-region. In each case, the QQ plots form a straight line, indicating that the sample data collected were drawn from the same distributions.**

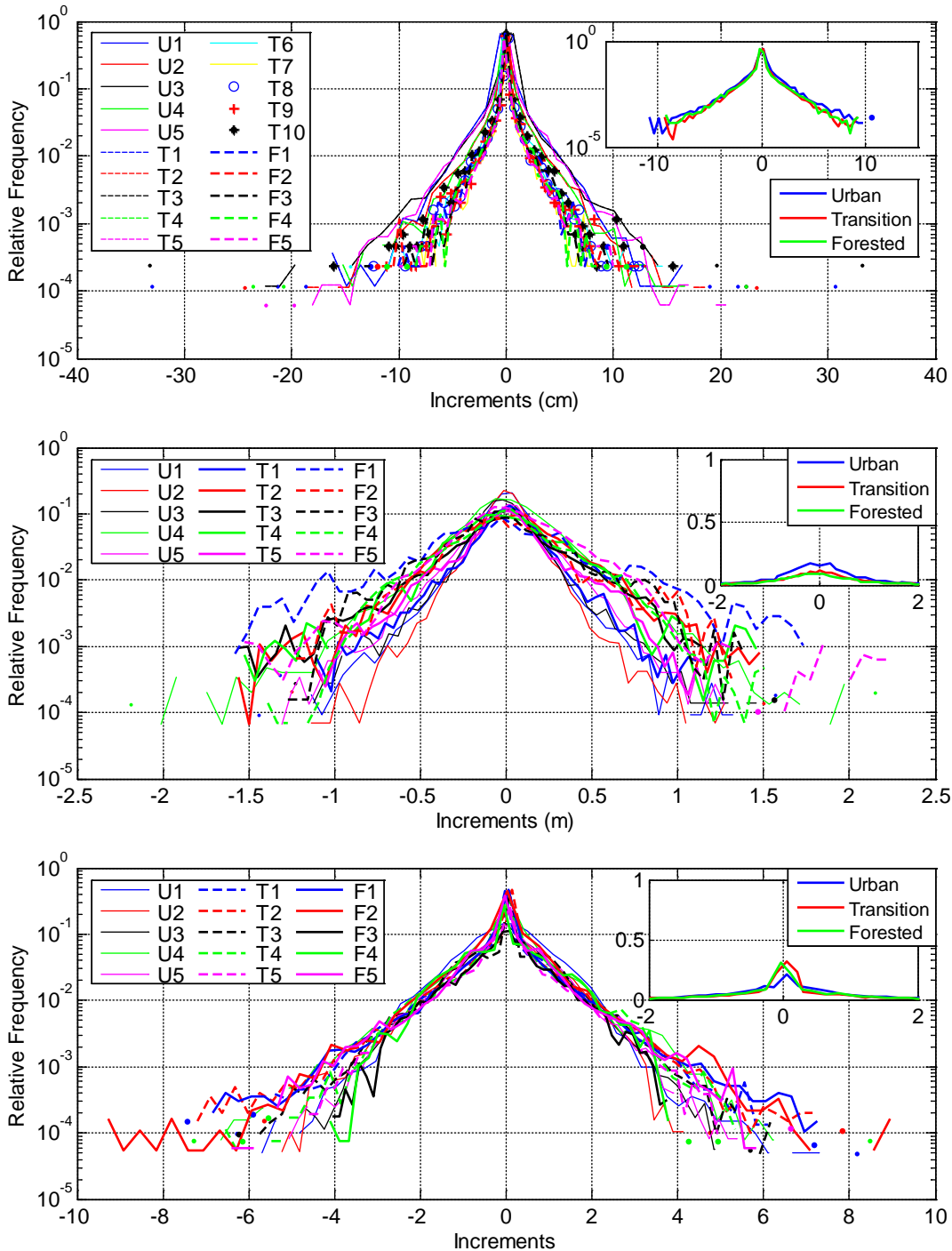


**Figure 9 – PDF increments for rainfall (top), groundwater elevation (center), and streamflow (bottom) with a scale equal to 365 days. The insets show the ensemble average of the PDF increments for each sub-region. Like Figure 7, the increments for streamflow are standardized. Notice how these PDFs are more symmetric compared to Figure 7.**

#### 4.1 Variability as a Function of Scale

By using spectral analysis, one can observe the variation intensities over a range of frequencies. The power spectral density (PSD) characterizes how the energy or the variance of a signal is distributed over a range of frequencies, or scales (Singh et al., 2014). Generally speaking, signals consist of a combination of minor signals of different sizes and characteristics. The power spectral density displays the frequencies in which the corresponding energy contributes to the original signal. Observations can be made to conclude which range of frequencies is strong or weak relative to the original signal. This information can be used to determine the frequencies in which these hydrologic processes are prevalent.

The power spectral density is expressed as follows:

$$\Phi(\omega) = \frac{1}{2\pi} \int_{-\infty}^{\infty} R(\tau) e^{-i\omega\tau} d\tau \quad (2)$$

where  $R(\tau)$  represents the autocorrelation function;  $\tau$  is time lag; and  $\omega$  is frequency (Stoica and Moses, 1997; Singh et al., 2010 and 2014; Guala et al., 2014; Keylock et al., 2014). The autocorrelation function can be further written as:

$$R(\tau) = \frac{E[(X_t - \mu)(X_{t+\tau} - \mu)]}{\sigma^2} \quad (3)$$

where  $E[\ ]$  denotes the expected value,  $\mu$  is mean,  $\sigma^2$  is variance, and  $t$  is time. Again, because there were multiple stations for each hydrologic process, the ensemble average power spectral densities over each sub-region were computed.

For rainfall, the PSD plots appear to be mostly linear for all sub regions. In Figure 10 (top), the slope for the urban sub-region is -1.07 and ranges from 2.5 to 10 days. High frequencies are associated with small time scales. Then, the slope slightly changes to -0.28,

ranging from 10 to 100 days. For the transition area in Figure 10 (center), the slope is much flatter, starting at -0.31 for frequencies of 2.5 days to 10 days. After that, the slope changes to -0.12, ranging from 10 to 100 days. Regarding the forested sub-region in Figure 10 (bottom), the slope at lower frequencies is -0.28, ranging from 2.5 to 10 days. At higher frequencies, this slope becomes -0.10, for frequencies ranging from 10 days to 100 days. The rainfall PSDs do not appear to show any major scaling breaks along the frequency spectrum. If anything, a minor scaling break is apparent at a frequency of 10 days. In fact, certain portions of the rainfall PSD plots in which the slopes are relatively flat can be characterized as spectral gaps, which are gaps that contain scales that do not contribute additionally to the energy variation (Singh et al., 2014). Rainfall variations, as observed before, stay mostly consistent throughout time, which could explain why the PSD plot appears flat.

Two spikes in the urban rainfall (Figure 10, top) PSD plot appear. These spikes have frequencies of roughly 3.3 and 6.7 days. This suggests that there are dominant frequencies of rainfall in which its energy or variance is very significant. Perhaps this may provide an indicator as to which specific rainfall events carry the most energy and more importantly, how this can impact the areas around the Everglades landscape, since they have to respond to this increase in energy. These frequencies may be associated with local storm events common in south Florida that have recurrence events ranging anywhere from a few days to one week. This information may be useful in assessing the hydrologic patterns being carried out along south Florida and can help in further protecting and maintaining the wetland ecosystems from further geomorphologic change.



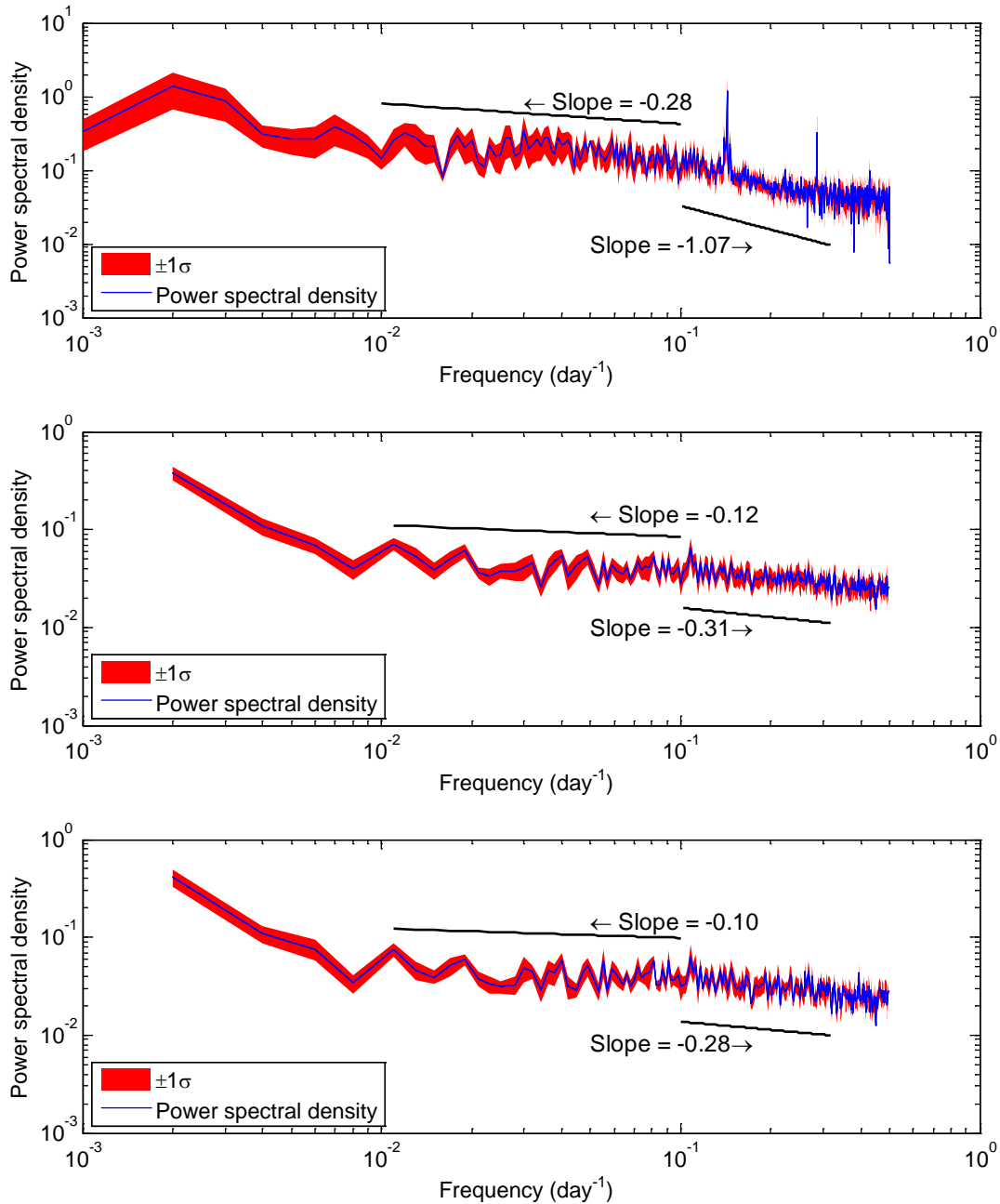


**Figure 10 – Average power spectral densities plotted with its error (shown as  $\pm 1$  standard deviation) for rainfall. The top, center, and bottom plots represent the urban, transition, and forested sub-regions, respectively.**

Figure 11 shows the ensemble average PSDs for  $G(t)$  for all three sub-regions. As can be seen from this figure, for all three sub-regions, the PSDs suggest a log-log linear behavior for a range of scales and, in fact, two different scaling regimes with a scaling break at a scale of  $\sim 10$  days. For example, looking at the urban sub-region, the slope of the PSD is  $-2.21$  at high frequencies (small time scales), ranging from 3 to 10 days. For larger time scales, the PSD slope reduces to  $-1.61$  for a range of 10 to 100 days, suggesting a decrease in correlation at larger time scales for  $G(t)$ . The PSD for the transition sub-region (Figure 11, center) has a slope of  $-2.18$  for higher frequencies (3 to 10 days) and  $-1.99$  for lower frequencies (10 to 100 days). As for the forested sub-region (Figure 11, bottom), the slope of the PSD has a value of  $-1.87$ . This slope slightly changes to  $-1.69$ , up to a scale of 100 days. Scaling regimes are classified as the linear portions observed in a log-log PSD plot (Singh et al., 2014). Note, that the scaling break (contrasting slopes at lower and higher frequencies) is more prominent in the case of urban as compared to forested sub-regions, and the difference between these PSD slopes for two different ranges mentioned above decreases from urban to forested sub-regions.

For streamflow,  $Q(t)$ , the PSD plots show similar behavior (i.e., two power-law scaling regimes, although the scaling break is shifted towards larger time scales,  $\sim 20$  days) to the  $G(t)$  PSD plots, shown in Figure 12. However, as expected and discussed above, an opposite trend is observed when moving from the urban to forested sub-regions. For example, the differences between the slopes of two scaling regimes in the PSD are 0.35, 0.40, and 0.90 for urban, transition, and forested sub-regions, respectively. This increase in slope difference for different sub-regions for the two scaling regimes suggests that the correlation in the larger scales decreases significantly as compared to smaller scales as the sub-region is changed from urban to

forested in the case of  $Q(t)$ . The scaling range where PSD slopes for  $Q(t)$  were computed was 4-20 days for smaller scales and 20-100 days for larger scales. Note that a similar scaling break in the range of 3 to 24 days in streamflow PSDs was observed by Pandey et al., (1998).

In the urban region, the PSD slope is -1.61, ranging from 4 days to about 20 days. Beyond this point, the PSD slope is -1.27, as shown in Figure 11 (top). For the transition sub region, the PSD slope found at high frequencies is -1.49, within the scales of 4 days and 20 days. At lower frequencies, the slope turns out to be -1.09, between scales of 20 days and 100 days. Lastly, for the forested sub region, the PSD slope at lower time scales is -2.71, between 4 days to 20 days. At more intermediate to higher time scales, the resulting slope is -1.61, ranging from 10 days to 100 days.

In addition, in the case for the transition and forested areas (Figure 12, center and bottom), three spikes in the PSD plots can be seen. In fact, the spikes correspond to a common frequency for the transition and forested sub-regions. These observed frequencies are at the scale of 7, 3.5 and 2.3 days, suggesting the presence of predominant wet seasons in South Florida which lasts from May to October, bringing with it the short duration events such as showers and thunderstorms occurring almost daily in the afternoons and evenings (Teegavarapu, 2012, 2013). It is speculated that the absence of such high energy peaks in the PSD in urban sub-region is due to the presence of manmade infrastructures such as canals or dams used for controlling or operating every few days, that smooths out these high and frequent fluctuations in  $Q(t)$ .

To further explore the transition in scaling regimes, the groundwater elevation and streamflow PSDs are superimposed, as shown in Figure 13. These PSDs are shifted in the vertical axis by order of magnitude for visualization purposes. Notice the scaling break for

groundwater is clearer in the urban sub-region, and becomes smoother as one approaches the forested sub-region (bottom row, left). The opposite is seen for streamflow. The scaling break is clearer in the forested sub-region, and smooths out approaching the urban sub-region. Again, this suggests that these processes are out of phase, or in other words, complement each other.

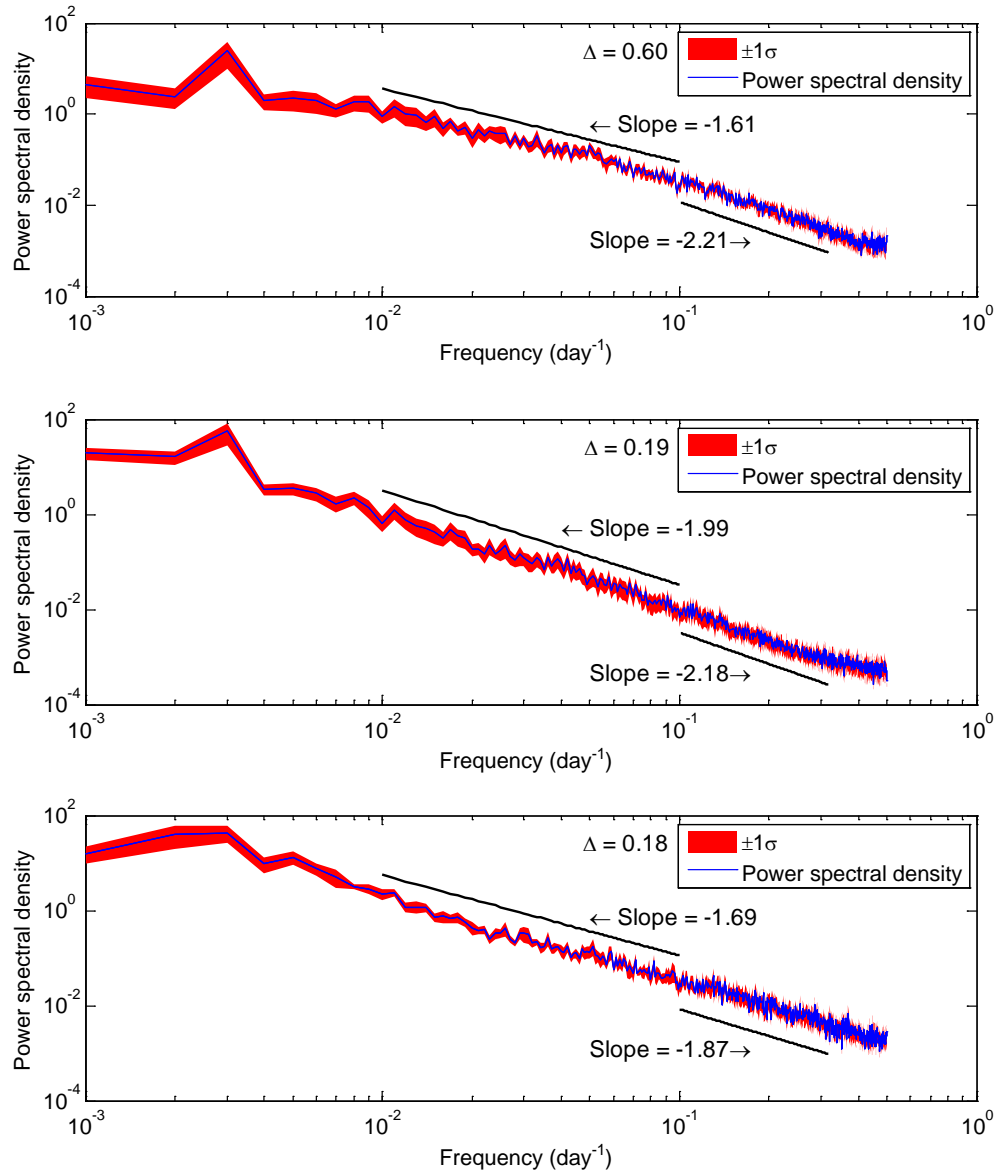


**Figure 11 – Average power spectral densities plotted with its error (shown as  $\pm 1$  standard deviation) for groundwater elevation. The top, center, and bottom plots represent the urban, transition, and forested sub-regions, respectively.**

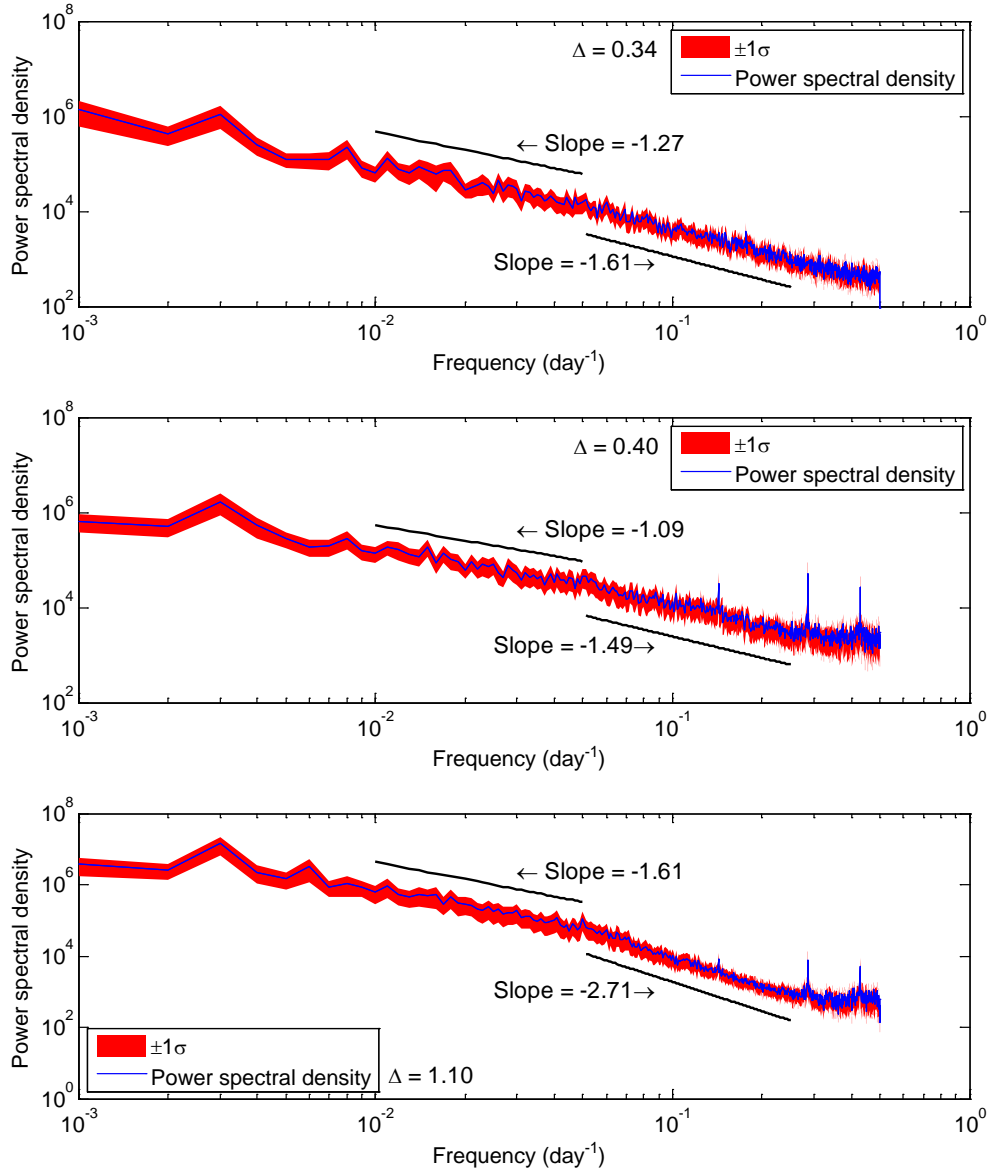


**Figure 12 – Average power spectral densities plotted with its error (shown as  $\pm 1$  standard deviation) for streamflow. The top, center, and bottom plots represent the urban, transition, and forested sub-regions, respectively.**

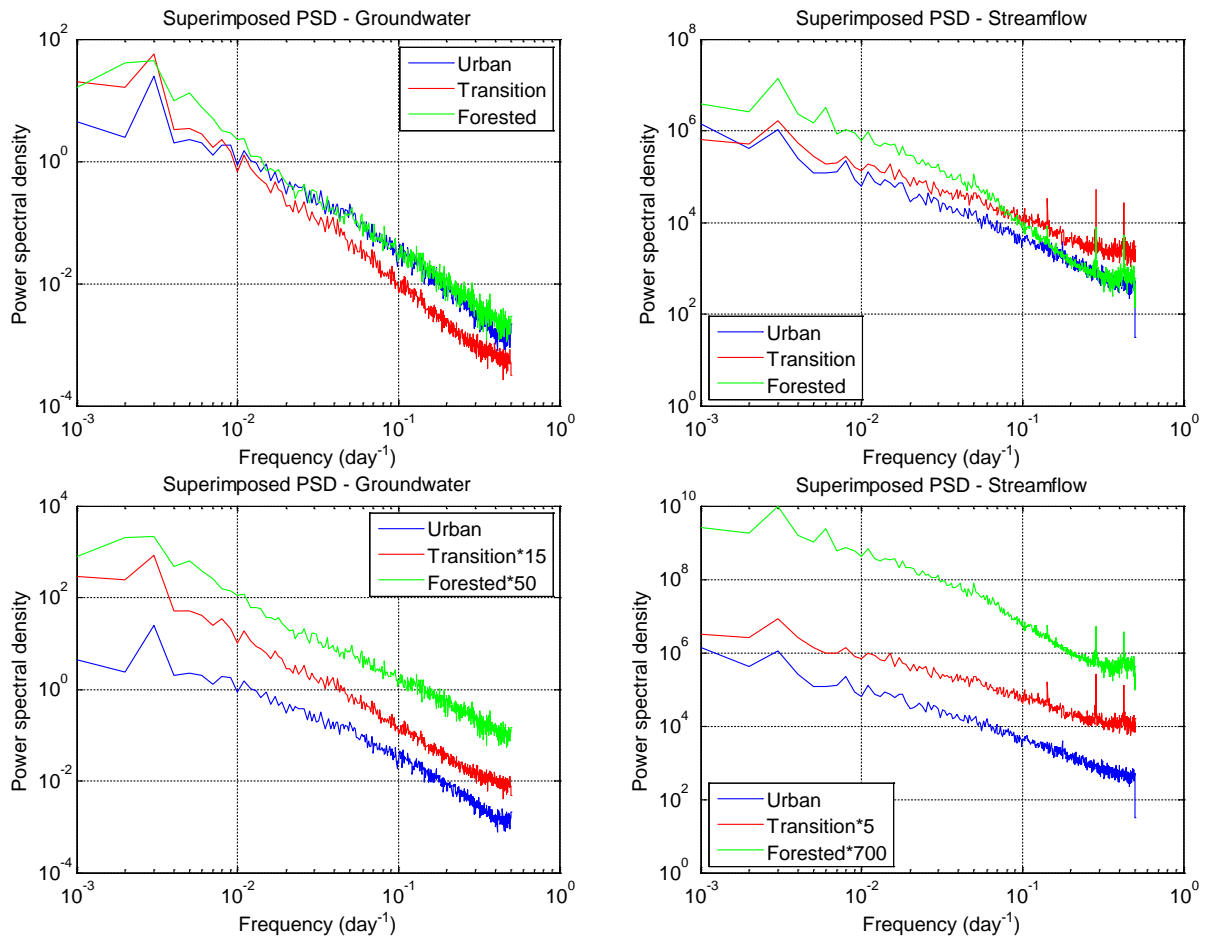


**Figure 13 – Superimposed power spectral density plots as is (top row), and shifted by several decades (bottom row). Notice the scaling nature of the plots changes as one moves from urban to forested and vice-versa.**

Note that all the PSD plots were computed using an ensemble average of different stations. To quantify the amount of uncertainty in the data, the area that represents one standard deviation above and below the mean is shaded. The red shaded areas in Figures 10-12 show  $\pm 1$  standard deviation. In some cases, namely for groundwater,  $G(t)$ , subtracting one standard deviation from the mean resulted a negative value, which cannot be represented in a log-log plot. To adjust for this, the ensemble mean was shifted one standard deviation above from its original position, then subsequently shading the area one standard deviation above and below the ensemble mean. As noticed from the red shaded areas, the amount of uncertainties in the data is relatively small for groundwater and streamflow. These uncertainties can be due to a combination of natural causes and as well as anthropogenic impacts.

#### 4.2 Mean, Variance, and Asymmetry as a Function of Scale

Obtaining the increments of the hydrologic processes allows one to analyze the processes from a stationary approach. This way, any statistics computed for the increments should characterize the processes in a more meaningful manner. However, instead of looking at one scale, or increment, these statistics can be computed across a range of time scales. This observation will reveal if there are any specific time scales in which relatively strong variability is observed. This analysis will focus on the mean, variance, and asymmetry across scales.

Differencing hydrologic time series serves to remove any non-stationarity and allows for more in-depth observations on the structure of these processes. Figure 14 shows the ensemble absolute mean computed across time scales. As expected, the mean of increments is close to zero. However, as scales increase, the magnitude of the mean increases slightly, which may infer that



certain scales are related to each other. Similarly, in Figure 15, the variance is computed across time scales. A similar behavior is observed among these plots. The variance tends to increase before undergoing a slight periodic behavior. This may suggest that these processes are related to each other at certain scales. For example, scales on the order of 1 or 2 years may reveal distinct signatures of obtained statistics of the hydrologic processes.

Exploring the asymmetry in the PDFs of increments, as observed in Figures 7 and 9, and its variations in different sub-regions could provide critical information about the Everglades experiencing major stresses and shifts. In fact, Guttal et al., (2008) argued that observing the changing skewness of the probability distributions of hydrologic processes provides an early and effective indication of a potential regime shift.

However, Figure 7 only shows the increments PDFs at one scale ( $a = 1$ ). Generally, physical variables such as  $R(t)$ ,  $G(t)$  and  $Q(t)$  have been shown to suggest strong variability across a range of scales as also seen in the PSD plots (Figure 10-12). To further explore the degree of asymmetry from the increment PDFs, one can compute the asymmetry index as a function of scale, defined as:

$$\text{Asymmetry Index, } A = \frac{\langle \Delta x(t, a)^3 \rangle}{\langle |\Delta x(t, a)^3| \rangle} \quad (4)$$

where the angled brackets denote a mean value. The asymmetry index  $A$  quantifies the degree of asymmetry as a function of scale (Singh et al., 2014).

To account for multiple stations and gauges (as in computing PSDs of rainfall, groundwater elevation, streamflow), for each sub region, the ensemble average was computed with respect to both process and sub-region.

Figure 16 shows the asymmetry index as a function of time scales for the hydrologic processes behaving in different manners. Both groundwater elevation,  $G(t)$ , and streamflow,  $Q(t)$ , behave similar to each other, as their asymmetry tends to decrease before undergoing a periodic behavior. Groundwater levels can dictate the extent of groundwater flow, or baseflow, occurring in an aquifer. Baseflow is a significant component of streamflow in South Florida, and is currently being impacted by factors, such as, pumping, drainage, and local topography (Finkl and Charlier, 2003). So, as groundwater levels are impacted in one way, streamflows respond in another manner, and vice-versa. This may suggest that groundwater elevation and streamflow are processes that are related to each other. Interestingly, a significant loss of variability in the asymmetry is observed for urban  $G(t)$ , whereas, for  $Q(t)$ , this loss occurs in the forested sub-region. The periodic sections have been normalized and included as insets in Figure 16. Each vector,  $X$ , was normalized using:

$$-1 + \left[ 2 \left( \frac{X - X_{\min}}{X_{\max} - X_{\min}} \right) \right] \quad (5)$$

There is no distinct pattern for rainfall (Figure 16, top) as scales increase, which means that rainfall doesn't vary much as a function of time scale, hence, its increments PDFs are symmetric.

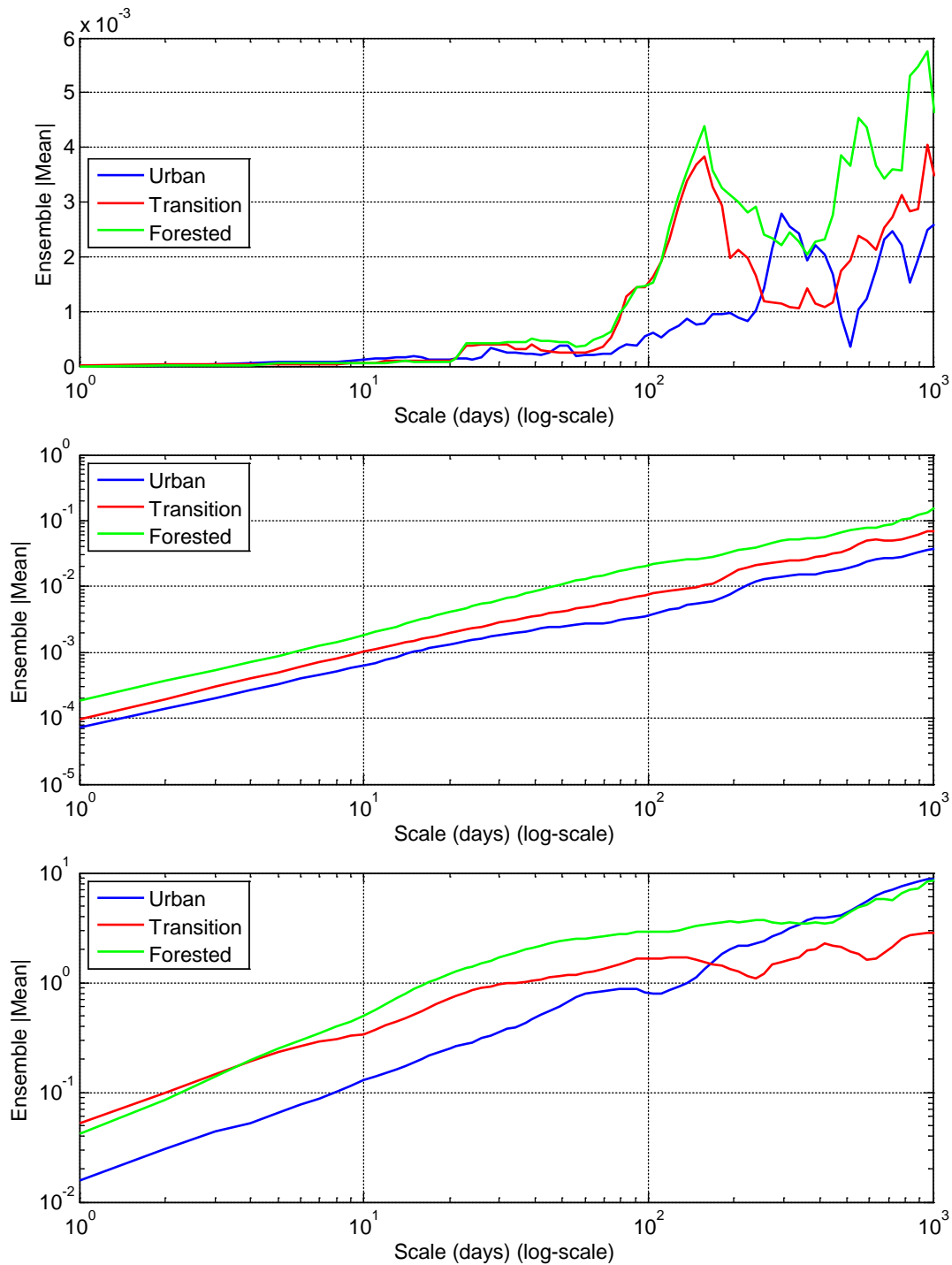


**Figure 14 – Average absolute mean across several scales for rainfall (top), groundwater elevation (center), and streamflow (bottom).**

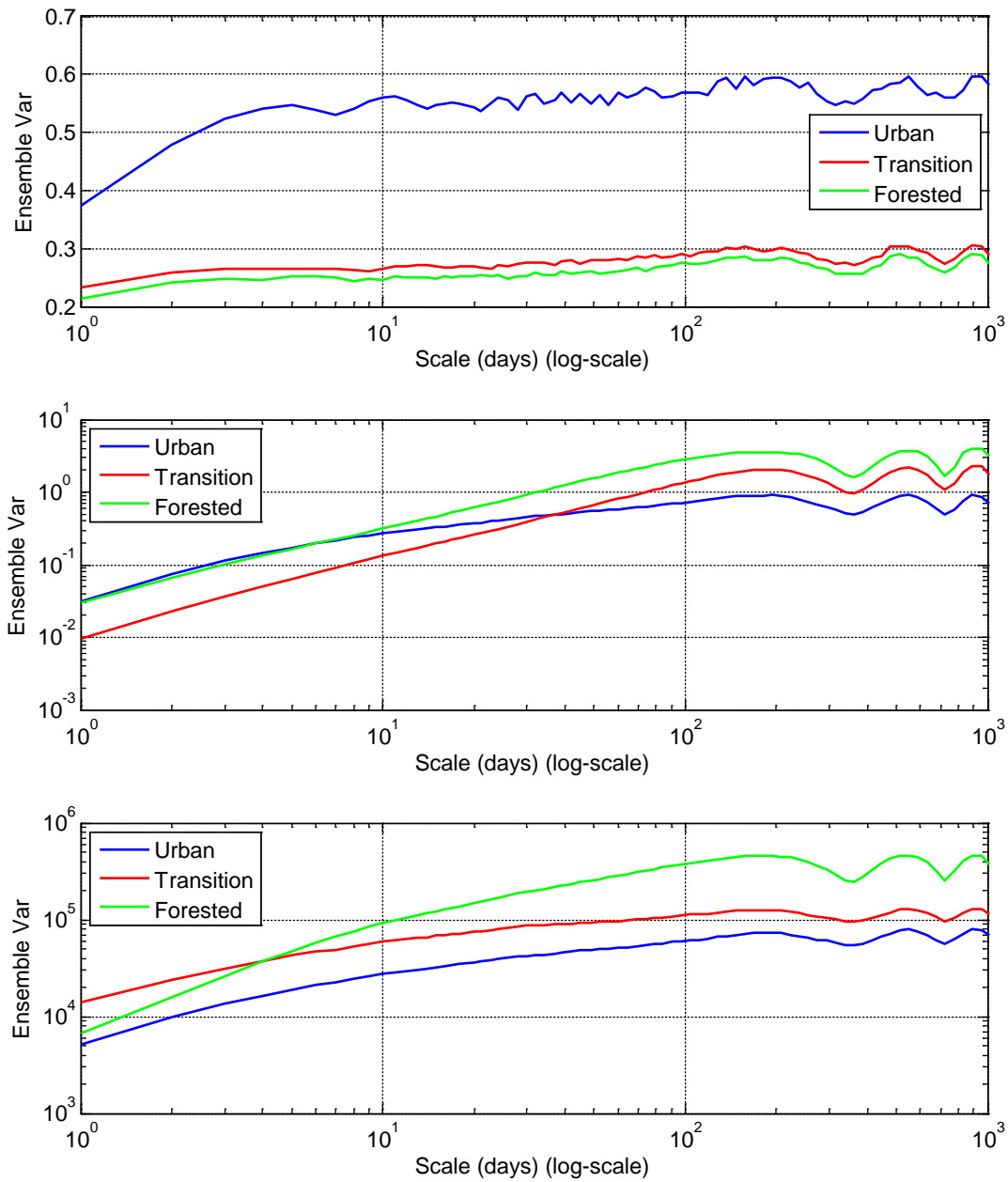


**Figure 15 – Average variance across several scales for rainfall (top), groundwater elevation (center), and streamflow (bottom).**

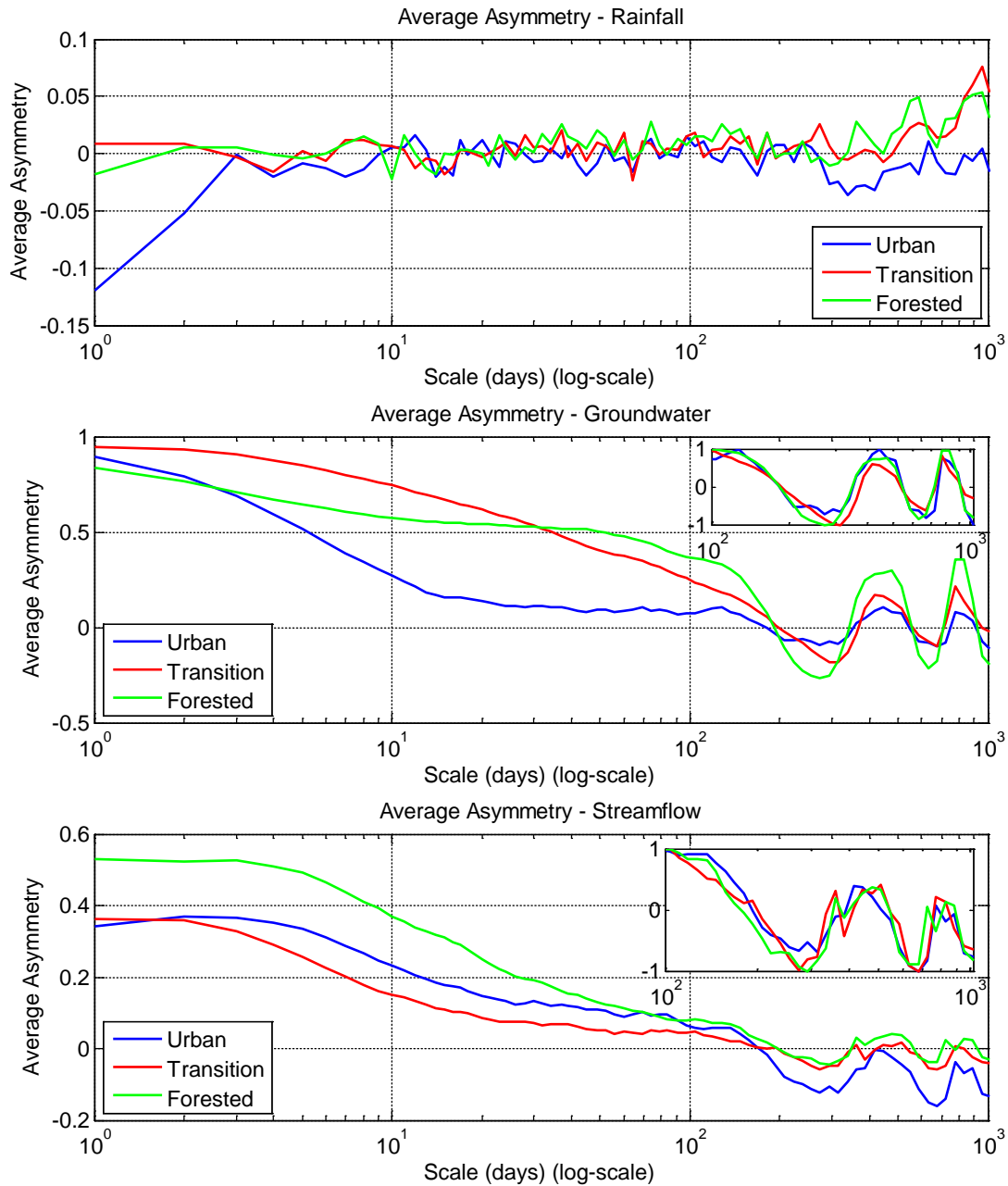


**Figure 16 – Average asymmetry (third moment) index across several scales for rainfall (top), groundwater elevation (center), and streamflow (bottom). The insets show the normalized versions of the periodicities that appear in the original plots for groundwater and streamflow.**

### 4.3 Interarrival Time

Observing the interarrival time distributions of the time varying processes allows one to quantify the mechanisms that are in place in these processes. In general, interarrival time refers to the time between events that arrive into the system exceeding a certain threshold. For this analysis, an ensemble of interarrival times (obtained from different locations for each sub-region) for rainfall,  $R(t)$ , groundwater elevation,  $G(t)$ , and streamflow,  $Q(t)$ , were computed for events exceeding the 5<sup>th</sup> and the 95<sup>th</sup> percentile thresholds, representing extreme events. Figure 17 shows the PDFs of interarrival times, displayed on log-log scale, for  $R(t)$ ,  $G(t)$ , and  $Q(t)$ , respectively. Interestingly these PDFs show a power-law behavior that can be expressed as a power-law function:

$$R(t) \sim t^{-\alpha} \quad (6)$$

where  $\alpha$  is the slope of the power function. Note that in some cases, there may have been a few significant outliers in the interarrival time data that prevented an appropriate power-law regression line from being plotted without drastically reducing the number of bins. To avoid this, these outliers were excluded.

As can be seen from Figure 17, the interarrival times for the three sub-regions show different power-law exponents. For example, comparing the urban and forested sub-regions for  $Q(t)$ , (Figure 17c, right), the power-law exponents are -2.05 and -1.32, respectively, implying that the interarrival time for the same frequency events is much shorter in the case of urban as compared to the forested sub-region. This is due to the fact the forested regions intercept runoff as groundwater and slow down the arrival of extreme events at the outlets.

In addition, comparing the slopes of interarrival times between the urban and forested sub-regions for  $G(t)$  and  $Q(t)$  with  $R(t)$ , the slopes for forested sub-region remains similar whereas for the case of urban sub-region,  $Q(t)$  and  $R(t)$  show similar slopes while the slope for  $G(t)$  increases, suggesting lower probability of higher extreme events in the case of urban sub-region for  $G(t)$ . This observation reinforces that the fact that significant anthropogenic influence in groundwater can alter landscapes. The power law exponents for all cases are listed in Table 2. Similar features are seen for the 5<sup>th</sup> percentile power-law regressions (Figure 17, left column). The rainfall regressions do not change, while the groundwater and streamflow regression slopes show changes in the way they are governed.

Essentially, observing the interarrival time distribution of these hydrologic processes further indicates that there are significant anthropogenic changes present around the Everglades. Perhaps if the degree or extent of the anthropogenic changes persists or amplifies, the natural regime of the hydrologic processes in the Everglades will soon be disrupted in such a way that the wetlands and the ecosystem cannot adequately respond to the adverse changes.

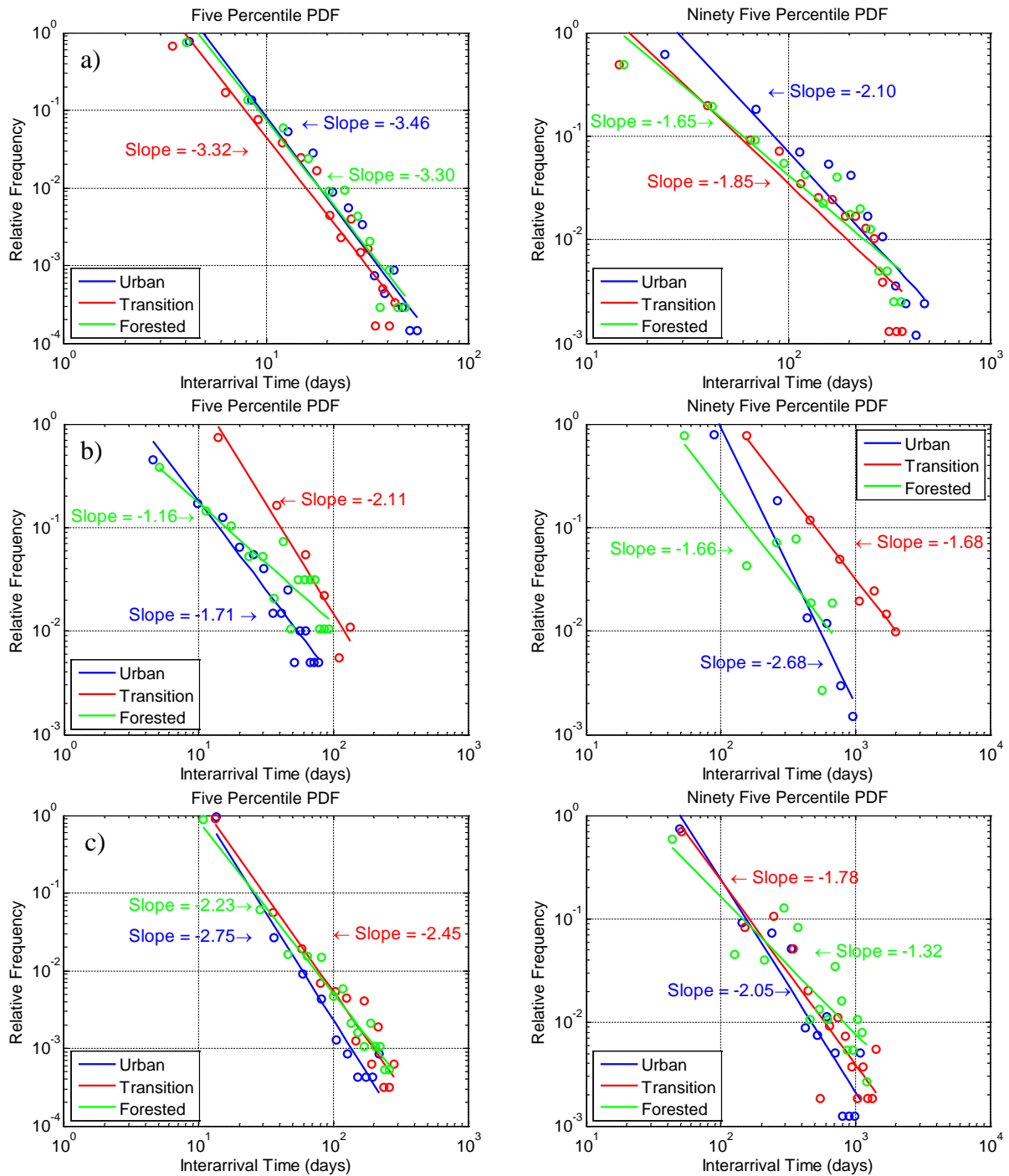


**Figure 17 – Five (left column) and ninety-five (right column) percentile PDFs for a) rainfall, b) groundwater elevation, and c) streamflow with power law fits for each area.**



**Table 2 – Power-law exponents of the interarrival PDFs listed from Figure 17.**

Slope, $\alpha$	Urban		Transition		Forested	
	5%	95%	5%	95%	5%	95%
Rainfall, $R(t)$	-3.46	-2.10	-3.32	-1.85	-3.30	-1.65
Groundwater, $G(t)$	-1.71	-2.68	-2.11	-1.68	-1.16	-1.66
Streamflow, $Q(t)$	-2.75	-2.05	-2.45	-1.78	-2.23	-1.32

#### 4.4 Effect of changing hydrology on river networks

The terrain of the Everglades and the greater south Florida region is mostly flat with the exception of the northwest section of the DEM (Figure 2). This area in north central Florida consists of a low ridge known as the Lake Wales Ridge, or the Mid-Florida range. This ridge spans about 242 km north to south. The ridge elevation spans from around 16-92 m above sea level. In the southern portion of Florida, where the Everglades reside, the land becomes flat, almost reaching sea level.

In modern investigations, digital elevation models (DEMs) are becoming increasingly useful in analyzing landscapes characteristics and features. These features such as river and channel networks, which interact with the above discussed hydrologic processes, can be extracted from DEMs, allowing investigators to observe how landscapes behave spatially and temporally (Tarboton et al., 1991; Hooshyar et al., 2016).

Figure 2 shows an example of the river network obtained from analyzing 30 m resolution DEMs for the Everglades and the greater south Florida region and provides a conceptual understanding of how the area is divided into different drainage basins and where the rivers ultimately discharge to. For example, in the lower regions of the Everglades, a collection of streams ultimately converge into one stream and eventually discharges at the southwest coast of Florida. The northern section of the Everglades discharges at the east coast of Florida. This particular flow regime appears to flow in the opposite direction compared to the historical flow regime. Note that due to the flat topographic nature of south Florida, working with 30 m DEMs may have limitations. Also, the presence of human intervention (i.e., in the form of man-made

canals, levees and water control structures) along the north end of the Everglades may lead to modified river networks.

Since our study categorizes the study area into three sub-regions, it is necessary to compare the river networks in each sub-region. For this purpose, within each sub-region, three drainage basins are mapped out and their drainage densities and local slopes were computed. The drainage density is defined as the total length of all the streams in a basin divided by the total area of the basin and characterizes how well or how poorly a basin is drained. Also note that the magnitude of drainage density is dependent on the resolution of the DEMs. This study is focused on the comparison of drainage density among different landscapes, and small channels may not be included due to the resolution of the DEMs (30 m). The ensemble averaged drainage density for each sub-region is listed in Table 3 along with the characteristics of the river network for each stream order,  $\Omega$ . As expected, drainage density decreases as one moves from the forested sub-region to the urban sub-region. Drainage basins in the forested sub-regions drain well, whereas the basins in the urban sub-regions drain poorly. Human interferences are a potential contribution to the lower drainage density in the urban sub-regions. Similar behavior is seen in the case of stream order based drainage densities, especially, for the 1<sup>st</sup>, 2<sup>nd</sup>, and 4<sup>th</sup> order basins. Comparing the local slopes across the three sub-regions, the slopes are roughly similar across the landscape due to the flat topographic nature of South Florida. This comparison can be seen in Figure 18. The urban, transition, and forested sub-regions had an average slope value of 2.60, 2.06, and 2.76 degrees respectively. The standard deviation of the slopes for the urban, transition, and forested areas are 2.97, 2.27, and 2.93 degrees respectively.

A clear indication of changes observed in this study in both hydrologic and geomorphic characteristics of the Everglades when comparing the urban and forested sub-regions suggest a significant influence of anthropogenic activities on the Everglades' landscape.

**Table 3 – Averaged basin and stream order characteristics for each sub region.**

<b>Region</b>	<b>Stream Order</b>	<b>Count</b>	<b>Length (km)</b>	<b>Area (km<sup>2</sup>)</b>	<b>Drainage Density (km<sup>-1</sup>)</b>	<b>Total Drainage Density (km<sup>-1</sup>)</b>
<b>Urban</b>	1	19.0	72.2	456.77	0.178	0.323
	2	12.3	47.8		0.095	
	3	2.7	13.4		0.036	
	4	4.0	18.6		0.021	
<b>Transition</b>	1	32.3	157.8	743.19	0.214	0.385
	2	17.3	57.1		0.078	
	3	7.3	38.8		0.056	
	4	8.3	31.0		0.037	
	5	1	0.1		0.001	
<b>Forested</b>	1	57.0	222.2	1373.91	0.254	0.525
	2	30.3	138.1		0.149	
	3	16.3	67.6		0.080	
	4	9.3	36.5		0.041	

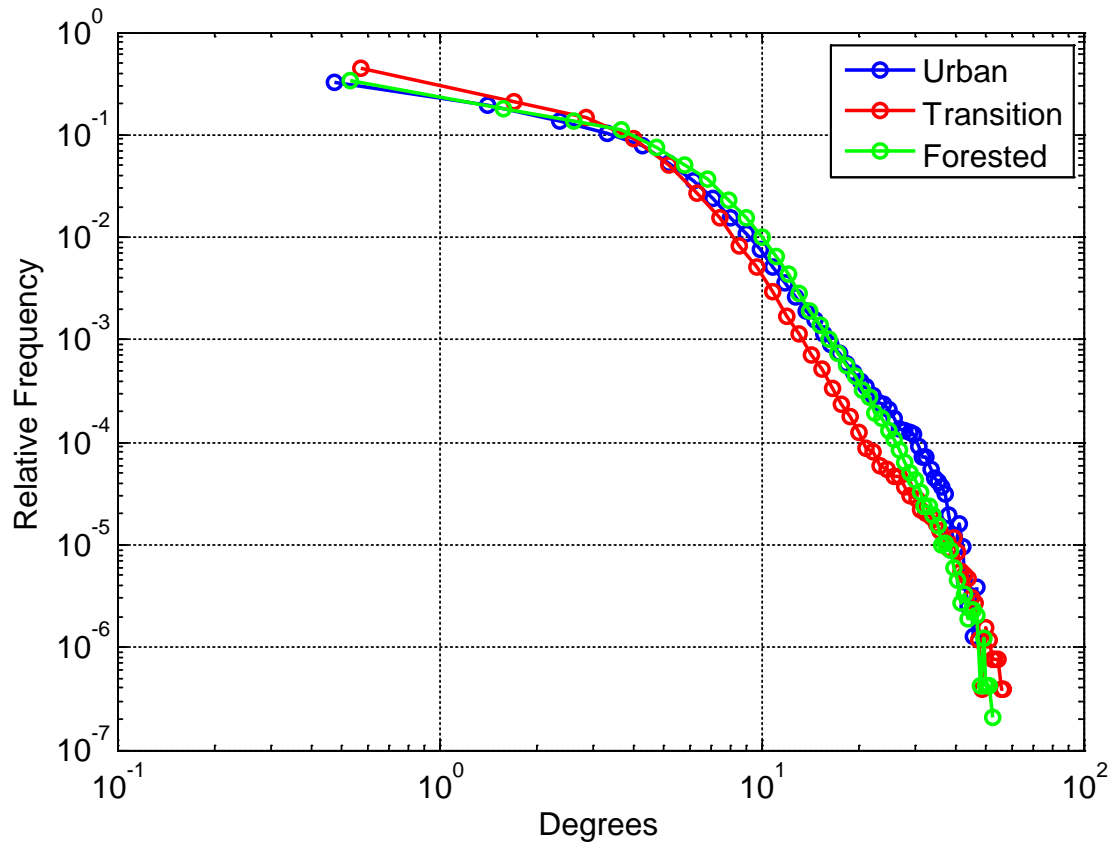


**Figure 18 – Slope PDFs of the sample watersheds for each corresponding area. These particular basins are shown in Figure 2.**

## CHAPTER 5: CONCLUSION

Wetlands host a diverse array of plant and animal species. The organisms depend on natural processes of the wetlands in order to carry out life processes and to survive and prolong their existence. This study explored changes in hydrologic and geomorphic processes that may have impacted the Everglades wetlands in some way, and argued how their signatures have changed spatio-temporally. In the presence of changing hydrologic processes, such as rainfall, groundwater elevation, and streamflow, the landscape has to adjust to a new dynamic equilibrium.

Changing skewness and asymmetry can serve as early warning indicators as to when a landscape may experience regime shifts (Carpenter and Brock, 2006; Guttal et al., 2008). In this case, regime shifts are detrimental in that it would cause the Everglades to deviate away from a stable state into another state. As the wetlands undergo this transition, many features and properties native or exclusive to the landscape, such as vegetation, tree and island connectivity, are lost or modified. Moreover, the aquatic and riparian species are victims to the morphologic changes and suffer degradations in ecosystems and habitats, which will prompt managing entities to anticipate the changing hydrology and protect the wildlife.

Analyzing hydrologic records and computing various statistics can provide useful insights as to how a certain location is changing over time. This type of procedure is adaptive in nature, so the conclusions obtained for one study can differ considerably for several landscapes in multiple locations (IPCC, 2001; Eckhardt and Ulbrich, 2003; Novotny and Stefan, 2006). Changes in one area may appear favorable for habitats whereas changes in another may appear

harmful to ecosystems. It is crucial that ecosystems be assessed in order to apply better management principles to protect and restore natural conditions that benefit the diverse wildlife.

Morphologic changes, although very minor and localized, can be observed from satellite imagery dating back to 1994-5. Analyzing the DEMs over the wetlands roughly show the distinct properties of the watersheds as one moves from the urban sub-region to the forested sub-region. As expected, the drainage density increases from urban areas to forested areas. This shows how human manipulation (i.e. urban development) influences the natural wetlands to some extent.

A collection of hydrologic data, in the form of rainfall, groundwater elevation, and streamflow, has been obtained and analyzed from stations in and around the Everglades wetlands. Higher order statistics were computed, (e.g., variance and asymmetry) as a function of time scale. These plots suggest distinct signatures of the urban, transition and forested sub-regions reconfirming the effects of human and climate on the ecosystem. For example, analyzing the power spectral density (PSD) plots reveals distinct scaling regimes across landscapes (urban to forested). In groundwater, scaling is more apparent in the urban region, whereas for streamflow, scaling is more apparent in the forested region, suggesting that these processes behave out of phase (complement) with each other. In other words, a significant difference in the slopes between smaller and larger scales of the PSDs is observed when transitioning from the forested to the urban sub-regions. The groundwater elevation and streamflow showed contrasting results.

The interarrival time analysis of extreme (>95<sup>th</sup> percentile) events showed power-law distributions for the three different sub-regions. In particular, comparing slopes of interarrival time PDFs between urban and forested sub-regions for  $G(t)$  and  $Q(t)$  with  $R(t)$ , the slopes for forested sub-region remains similar whereas for urban sub-region,  $Q(t)$  and  $R(t)$  show similar



slopes while the slope for  $G(t)$  increases, suggesting lower probability of higher extreme events in the case of urban sub-region for  $G(t)$ . This observation reinforces the fact of significant anthropogenic influence on groundwater in the Everglades can alter landscapes.

These results suggest that any further accelerated changes in climatic and anthropogenic activities can change the dynamic nature of the Everglades and can pose a threat to the landscape and ecosystem. This assessment raises the need to restore natural conditions and regulating anthropogenic activities so that its effects are not significant.

## LIST OF REFERENCES

- Abed-Elmdoust, A., Miri, A., and Singh, A. (2016). "Reorganization of river networks under changing spatio-temporal precipitation patterns: an optimal channel network approach." *Water Resources Research*. <http://dx.doi.org/10.1002/2015WR018391> (In press).
- Carpenter, S. R., and Brock, W. A. (2006). "Rising variance: a leading indicator of ecological transition." *Ecology Letters*, 9(3), 311-318.
- Chambers, L. G., Davis, S. E., and Troxler, T. G. (2015). "Sea level rise in the Everglades: Plant soil-microbial feedbacks in response to changing physical conditions". *Microbiology of the Everglades ecosystem*. CRC Press, Boca Raton, FL. p.89-112.
- Davis, S.M., Gunderson, L.H., Park, W.A., Richardson, J.R., and Mattson, J.E. (1994). "Landscape dimension, composition, and function in a changing Everglades ecosystem." In: Davis, S.M., Ogden, J.C. (eds) *Everglades: The ecosystem and its restoration*. St. Lucie, Delray Beach, pp 419–444.
- Eckhardt, K., and Ulbrich, U. (2003). "Potential impacts of climate change on groundwater recharge and streamflow in a central European low mountain range." *Journal of Hydrology*, 284, 244-252.
- Erwin, K.L. (2009). "Wetlands and global climate change: the role of wetland restoration in a changing world. *Wetlands Ecology and Management*, 17 (1), 71-84.
- Finkl, C. W., and Charlier, R. H. (2003). "Sustainability of subtropical coastal zones in southeastern Florida: Challenges for urbanized coastal environments threatened by developments, pollution, water supply, and storm hazards." *Journal of Coastal Research*, 19, 934-943.

- Guala, M., Singh, A., BadHeartBull, N., and Fofoula-Georgiou, E. (2014). "Spectral description of migrating bedforms and sediment transport." *Journal Geophysical Research*, 119 (2), 123-137, doi:10.1002/2013JF00275.
- Guttal, V., and Jayaprakash, C. (2008). "Changing skewness: an early warning signal of regime shifts in ecosystems." *Ecology Letters*, 11, 450-460.
- Hooshyar, M., Wang, D., Kim, S., Medeiros, S. C., and Hagen, S. C. (2016). "Valley and channel networks extraction based on local topographic curvature and k-means clustering of contours." *Water Resources Research*, 52, doi:10.1002/2015WR018479.
- IPCC, (2001) In: Houghton, J.T., Ding, Y., Griggs, D.J., Noguera, M., van der Linden, P.J., Dai, X., Maskell, K., and Johnson, C.A. (Eds.), *Climate Change 2001: The scientific basis. Contribution of Working Group I to the Third Assessment Report of the Intergovernment Panel on Climate Change*, Cambridge University Press, Cambridge, UK.
- Keylock, C. J., Singh, A., and Fofoula-Georgiou, E. (2014). "The complexity of gravel bed river topography examined with gradual wavelet reconstruction." *Journal of Geophysical Research*, 119 (3), 682-700, doi:10.1002/2013JF002999.
- Kleinen, T., Held, H., and Petschel-Held, G. (2003). "The potential role of spectral properties in detecting thresholds in the earth system: application to the thermohaline circulation." *Ocean Dynamics*, 53, 53-63.
- Larsen, L. G., Aumen, N., Bernhardt, C., Engel, V., Givnish, T., Hagerthey, S., Harvey, J., Leonard, L., McCormick, P., McVoy, C., Noe, G., Nungesser, M., Rutchey, K., Sklar, F., Troxler, T., Volin, J., and Willard, D. (2011). "Recent and historic drivers of landscape change in the Everglades ridge, slough, and tree island mosaic." *Critical Reviews in*

*Environmental Science and Technology*, 41(S1), 344-381. doi:

10.1080/10643389.2010.531219.

Larsen, L. G., Choi, J., Nungesser, M., and Harvey, J. (2012). "Directional connectivity in hydrology and ecology." *Ecological Applications*, 22(8): 2204-2220.

Larsen, L. G., and Harvey, J. W. (2010). "How vegetation and sediment transport feedbacks drive landscape change in the Everglades and wetlands worldwide." *The American Journalist*, 176: E66-E79.

Larsen, L. G., Harvey, J. W., and Crimaldi, J. P. (2009). "Predicting bed shear stress and its role in sediment dynamics and restoration potential of the Everglades and other vegetated flow systems." *Ecological Engineering*, 35, 1776-1785.

Larsen, L., Moseman, S., Santoro, A. E., Hopgensperger, K., and Burgin, A. (2010). "A complex-systems approach to predicting effects of sea level rise and nitrogen loading on nitrogen cycling in coastal wetland ecosystems." *Eco-DAS*, 8, 67-92.

Noe, G. B., Harvey, J. B., Schaffranek, R. W., and Larsen, L. G. (2009). "Controls of suspended sediment concentration, nutrient content, and transport in a subtropical wetland." *Wetlands*, 30, 39-54.

Nourani, V., Nezamdoost, N., Samadi, M., and Vousoughi, F. D. (2015). "Wavelet based trend analysis of hydrological processes at different time scales." *Journal of Water and Climate Change*, 6(3), 414-435.

Novotny, E. V., and Stefan, H. G. (2006). "Stream flow in Minnesota: Indicator of climate change." *Journal of Hydrology*, 334, 319-333.

- Ogden, J.C., (2005). "Everglades ridge and slough conceptual ecological model." *Wetlands*, 25, 810–820.
- Pandey, G., Lovejoy, S., and Schertzer, D., (1998). "Multifractal analysis of daily river flows including extremes for basins of five to two million square kilometres, one day to 75 years." *Journal of Hydrology*, 208, 62-81.
- Scheffer, M., Carpenter, S., Foley, J. A., Folke, C., and Walker, B. (2001). "Catastrophic shifts in ecosystems." *Nature*, 413, 591-596.
- Singh, A., Porté-Agel, F., and Foufoula-Georgiou, E. (2010). "On the influence of gravel bed dynamics on velocity power spectra." *Water Resources Research*, 46, W04509, doi: 10.1029/2009WR008190.
- Singh, A., Howard, K. B., and Guala, M. (2014). "On the homogenization of turbulent flow structures in the wake of a model wind turbine." *Physics of Fluids*, 26, 025103, doi: 10.1063/1.4863983.
- Singh, A., Reinhardt, L., and Foufoula-Georgiou, E. (2015). "Landscape reorganization under changing climatic forcing: Results from an experimental landscape." *Water Resources Research*, 51(6), 4320-4337, doi:10.1002/2015WR017161.
- Sklar F., McVoy, C., VanZee, R., Gawlik, D. E., Tarboton, K., Rudnick, D., Miao, S., and Armentano, T. (2002). "The effects of altered hydrology on the ecology of the Everglades." In: Porter, J.W., Porter, K.G. (eds) *The Everglades, Florida Bay, and coral reefs of the Florida Keys: An ecosystem source book*. CRC, Boca Raton, pp 39–82.
- Sophocleous, M. (2002). "Interactions between groundwater and surface water: the state of the science." *Hydrogeology Journal*, 10, 52-67.

Stoica, P., and Moses, R. L. (1997). Introduction to spectral analysis, Prentice Hall, Upper Saddle River, N. J.

Tarboton, D. G., Bras, R. L., Rodriguez-Iturbe, I. (1991). "On the extraction of channel networks from digital elevation data." *Hydrological Processes*, 5, 81-100.

Teegavarapu, R.S.V. (2012). Floods in a changing climate: Extreme precipitation, *Cambridge Univ. Press*, Cambridge, U. K.

Teegavarapu, R. S. V. (2013). "Climate change-sensitive hydrologic design under uncertain future precipitation extremes." *Water Resources Research*, 49, 7804–7814, [doi:10.1002/2013WR013490](https://doi.org/10.1002/2013WR013490).

Winter, T. (1999). "Relation of streams, lakes, and wetlands to groundwater flow systems." *Hydrogeology Journal*, 7, 28-45.